Maritime Use Case: Requirements, Scenario Definition and Initial Evaluation Report
Work Package 3 Tasks 3.1-3.3 Deliverable D3.2

Authors

Raffaele Grasso, Gabriele Ferri, Elena Camossi, Alessandro Faggiani
CMRE

Dimitris Zissis, Konstantina Bereta, Konstantinos Chatzikokolakis, Ioannis Kontopoulos, Marios Vodas
MarineTraffic

Distribution list:

Group:	Others:
WP Leader: MarineTraffic (MT) Task Leader: MarineTraffic (T3.1, T3.3), CMRE (T3.2)	Internal Reviewer: RapidMiner GmbH INFORE Management Team INFORE Project Officer

Document history:

Revision	Date	Section	Page	Modification
0.1	28/05/20	1-2	1-8	Introductory Material
0.4	15/06/20	3-8 Appendix I Appendix II	All	First Draft
0.5	22/06/20	-	-	Internal Review Comments
0.7	23/06/20	All	All	Incorporation of reviewer comments
0.9	24/06/20	Appendix III	56-76	Expert Users Questionnaires
1.0	26/06/20	-	-	Final Version

Approvals:

First Author: Raffaele Grasso (CMRE) Date: 15/06/2020

Internal Reviewer: Fabian Temme (RapidMiner) Date: 22/06/2020

Coordinator: Antonios Deligiannakis (Athena) Date: 29/06/2020

Table of contents:

1 Executive Summary

This report summarises the results of the preliminary evaluation of the components developed for the Maritime Use Case that will be integrated and tested in a final experimentation at sea toward the end of the Project INFORE.

The Maritime Use Case consists in developing and deploying a hybrid sensor network for ship target detection, localization and classification. Sensor data for the global scale and the local scale surveillance scenario, resulting in an extreme scale data stream, will be integrated in a maritime situation awareness platform to perform high level fusion tasks and target behavioural analysis in order to detect behavioural anomalies of vessels with respect to the normal traffic in the area of interest. The developed platform will be integrated/using the INFORE architecture, utilizing its capabilities to analyse extreme scale streamed data.

The evaluation is performed using a set of key performance indices (KPIs) defined for the single components of the system and for the system as a whole, including human factors. The data used in the evaluation process are historical data available at the beginning of the Project INFORE or generated by simulating surveillance scenarios.

The tested components include i) the CMRE coordinated sea surface robotic sensor network for target detection and localization by acoustic data, the target detection and classification systems for satellite data and for thermal and RGB video camera data, and the MarineTraffic situation awareness platform algorithms for complex event detection.

The results of the evaluation are in general in line with the expectations. The coordinated robotic sensor network outperforms the base network without coordination, the classification from satellite data and camera data performs with classification accuracy around or greater than 90% and around 80%, respectively. The complex event classifier system has analogous performance with accuracy achieving, in some cases, values greater than 90%.

The report provides a complete description of each component, including theoretical details, the evaluation of the components and finally a preliminary plan of the final experiment at sea to evaluate the Maritime Use Case as a whole.

Future work before the final experiment includes implementation of the control and cooperation software on board the surface robot vehicles and further test of the classification algorithms for satellite and camera data and for complex events. Furthermore, the detailed plan, including logistic aspects, of the final experiment at sea will be started soon this year and finalized next year.

2 Introduction

2.1 The maritime use case

The Maritime Situational Awareness (MSA) is the capability of understanding events, circumstances and activities impacting the maritime environment. MSA is essential for the preparation, the prevention and the potential required reaction to provide a sustainable stable environment. The objectives of this use case are the following: (i) the development of workflows for the automatic detection, localisation and classification of targets of interest and their behaviour (maritime events), and (ii) the utilisation of a network of heterogeneous mobile sensorised platforms which, based on the inferred MSA knowledge, will be able to closely investigate the potential dark targets i.e. targets that are temporarily not observable by cooperative target sensors such as the Automatic Identification System (AIS).

The fusion of heterogeneous streams of data plays a significant role in acquiring a complete picture of the Maritime domain. The different sources of data (see Appendix I for a detailed description) that we use in INFORE are the following:

- AIS data
- Satellite data
- Acoustic data
- Thermal/video camera data

The data from the sensors are processed in order to detect the presence of suspect targets in a given area of interest and estimate their position and identity attributes. This information from the field is transmitted to a situational awareness platform that performs high level fusion tasks and the analysis of the target behaviour to detect possible behavioural anomalies.

This report is devoted to provide a preliminary evaluation of the single components of the use case and of the situational awareness platform using existing data and simulations, in preparation to the final pilot experiment at sea where the designed hybrid sensor network will be deployed and linked to the situational awareness platform. The experiment will provide final evaluation, using both quantitative metrics and qualitative human factors criteria, and new data sets, including ground-truth data that will be used to improve the system in future work. Because the performance of single components of the system affect the performance of the system as a whole, the approach followed in the Project and by converse in this report, is bottom up, starting from the single component evaluation and going to the evaluation of the complete use case system.

The report is organised as follows: this introduction will provide in the next subsections a brief overview of the components which are going to be evaluated and the list of key performance indicators (KPIs) on which the evaluation is based. Section 3 describes the field sensors used in the project, the so called local view sensors, the algorithms for target detection, localization and classification, and reports the results of the performance evaluation on previous data sets and simulations. Analogously, section 4 reports performance evaluation of those sensors providing more contextual information at global scale. Section 5 describes the platform for situational awareness and provides preliminary performance figures as well. Section 0 shows a preliminary plan of the final pilot experiment at sea and section 0 draws conclusions and traces the way ahead.

Technological components, short introduction

The maritime use case is based on the following technological components (see Figure 1 for a schematic summary):

1) A hybrid network of dynamic and static sensor for the local view that provides real time observations in a limited area of interest of cooperative as well as non-cooperative targets.
2) A set of sensors for the global view to observe a wider area and provide contextual information.
3) A platform for situational awareness that integrates data and information streams
from the local and global view sensors and analyses the behaviour of single surface targets as well as of the global vessel traffic surrounding them.

These components will be integrated and tested during the real pilot experiment at sea whose execution plan will be detailed in section 0. The single components will be described section 3, 4 and 5 and evaluated in terms of KPIs using simulated and available real data.

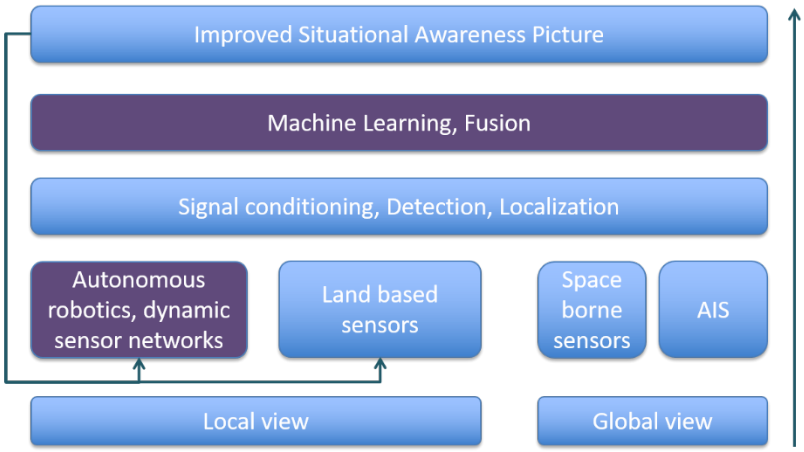

Figure 1: Schematic of the Maritime Use case components.

2.2 Evaluation

The evaluation of the Maritime Use Case is based on the definition of a series of KPIs for the single sensor components of the use case and for the situation awareness platform that integrates information from the single components and performs high levels data fusion and analysis tasks. The KPIs for the situation awareness platform are in turn defined for performance and accuracy evaluation, and for human factor evaluation. The KPIs will be evaluated using simulated scenarios and available data for both the single sensor components and the situation awareness platform, and during a final pilot experiment described in the final part of the document. The KPIs will be described in more details in the following paragraphs.

2.2.1 KPIS for target localization and classification

The KPIs for target classification from satellite and thermal camera data include the classification accuracy, i.e. the percentage of correct classified input samples with respect to the total number of samples of the training and validation sets and the receiving operating characteristic curves (ROC) for binary classifiers (e.g. a classifier for detecting ship and non-ship objects) that is a graph of the false positive rate vs the true positive rate. The classifier performance is the higher as the greater the area under the ROC curve is, ideally approaching the maximum value of 1 which is the perfect case of a classifier with 100% accuracy and 0 false alarm rate.

The robotic cooperative sensor network for target detection and localization will be evaluated using three KPIs. The first one is the target acquisition time which is the time needed by the network to confirm that a target, entering the surveilled area, is actually acquired. The second parameter taken into account is the time on target that is the total amount of time the network is able to observe a confirmed target within the time frame where the target is present. This KPI is linked with the third parameter that is the probability of detection i.e. the probability the network is able to detect the target in the hypothesis that the target is present. The KPIs are evaluated to compare a base model that is the network without cooperative behaviour vs the network with cooperative behaviour. The KPIs will be evaluated using simulated data as reported in the next sections and during the final pilot experiment.

2.2.2 KPIs for situational awareness and event prediction

In this section we describe the KPIs for the MSA Use Case of INFORE to evaluate the performance of the situational awareness platform. We group the KPIs into two categories. The first category includes the KPIs that are quantitative and measurable using ground truth datasets and experiments. The second category includes the human factor evaluation KPIs. In order to measure these KPIs, experts should be contacted, asked to perform certain scenarios, and interviewed for their feedback. These KPIs should be assessed taking into consideration the behaviour of experts during the execution of the scenarios (e.g., how many steps did they need to complete a tasks, how many mistakes they made, etc.) in comparison to approaches they already use to perform the same tasks in their jobs. The respective KPIs are described in Table 1 and Table 2.

Table 1-KPIs related to accuracy and performance

KPIs		Validation
1.1	Above 80% accuracy in target detection (from data fusion).	Experiments using ground truth datasets
1.2	Above 80% in complex maritime event detection and forecasting.	
1.3	Fusion of at least three different streams of data (2 global, 1 local)	
1.4	Maritime event detection/forecasting in sub-second time	

Currently, we have accomplished KPIs 1.1, 1.3 and partially the KPIs 1.2 and 1.4. The reason for this is that the integration for the complex event forecasting component of NCSR will be carried out in the following months, when we will be able to conduct the respective experimental evaluation. The second set of KPIs are mostly related to the evaluation of the final version of the INFORE platform, when all integration tasks are completed. Even though we contacted experts, presented our current results to them and received feedback, it is mostly related to the individual components that were developed in the project so far. We expect that in D3.3 experts will be able to execute complex MSA workflows using the Graphical Editor component of the INFORE Architecture and compare the INFORE solutions to the way they execute the same (or similar) workflows in their day-to-day tasks.

Table 2-KPIs for the human factor evaluation

KPIs		Validation
2.1	Functionality: the system should have the functionality the user expects (see requirements defined in D3.1)	The user will be asked to complete some scenarios defined in D3.1 and the interviewer will monitor their interaction with the system. Then, the user will be interviewed. He will be asked to rate the INFORE solutions presented to them comparing them to how they perform the same workflows in their day-to-day tasks. The INFORE workflows should achieve better ratings than existing solutions.
2.2	Interpretability of results: The user should be able to understand the results displayed to them.	
2.3	Overall system usability: The system should be easy to use for the user.	
2.4	Trust: The user should trust that the information presented to them is accurate.	

3 Sensor network for the local view

The hybrid sensor network used for the local area surveillance scenario (local view) includes a dynamic network of two wave-gliders autonomous surface robots equipped with passive acoustic sensors for cooperative surface target detection and localization, and a land based thermal camera aided by a co-located RGB camera for target detection and classification. This section provides details on the algorithms for cooperative target detection and localization by the robotic network, a brief description on target classification using multi-modal video camera deep learning algorithms and a final part on the options that will be considered in the final piloting experiment for local sensor integration including centralized to fully distributed approaches.

3.1 Passive acoustic cooperative target localization by a network of surface robots

The passive sonar robotic network concept is sketched in Figure 2. Wave-glider surface autonomous vehicles are equipped with volumetric passive sonar sensors for surface target detection and localization which are able to provide target bearing (direction of arrival) measurements after a beamforming processing of the acquired signal. The communication between the vehicles and a remote Command and Control centre (on a mother ship or on land) are guaranteed by continuous air/satellite communication and optionally by underwater communication modems. Wave-gliders have been selected due to their long-endurance and quiet navigation.

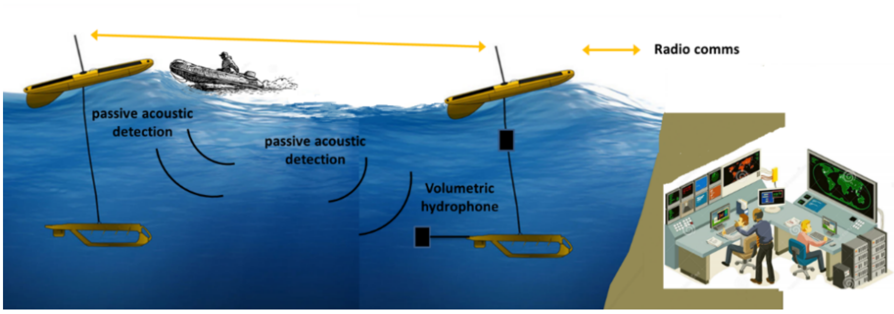

Figure 2: Concept of the multi-robot, persistent, passive monitoring network for surface target detection and localisation. Adapted from a LiquidRobotics picture [41].

The PERSEUS sensor (see Figure 3) will be mounted on board each vehicle. The sensor is a passive volumetric array composed of 8 hydrophones that are used to estimate the target bearing. The sensor has been tested recently at sea in La Spezia using a rubber boat as a test target performing different trajectories at different speeds. The signal received from the target is under analysis. A preliminary evaluation of the sensor performance is reported in the following sections.

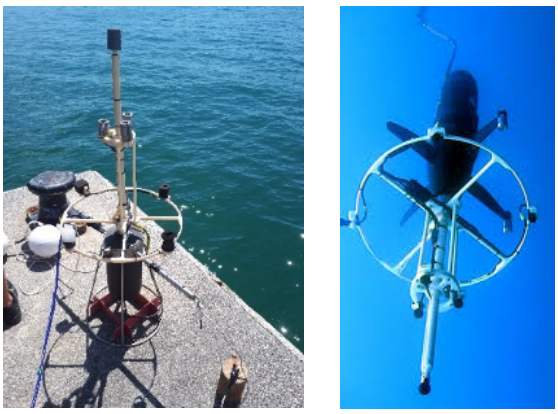

Figure 3: the PERSEUS sensor

At a higher level of cooperation, the surface vehicles, each one being a node of the surveillance network, exchange information to coordinate the nodes activities. The mission for the node robots can be divided into two phases (Figure 4): area survey and target cues exploitation. The mission starts with the vehicles operating in the area survey phase.

Their objective is to guarantee the monitoring of an area. Some mission objectives have to be guaranteed on the assigned region, for instance on the cumulative probability of target detection as proposed in [1], or on the probability of target presence given the collected measurements. The problem is intrinsically dynamic, due to the mobility of the target. For this reason, the vehicle objectives also include a temporal dimension. The region has to be covered periodically, since a target can enter in regions already surveyed.

When some cues about the target are produced by the on-board signal processing chain, the target cues exploitation phase begins. The wave-gliders now control their position to facilitate the target localisation. Fusing the bearing measurements allows them to estimate the target position and to adapt their navigation accordingly. This phase ideally culminates with the target confirmation and with the communication of its presence and position to the Command and Control Centre. If cues are recognised as a false alarm, or the target has moved too far for being detected, the system switches back to the area survey phase.

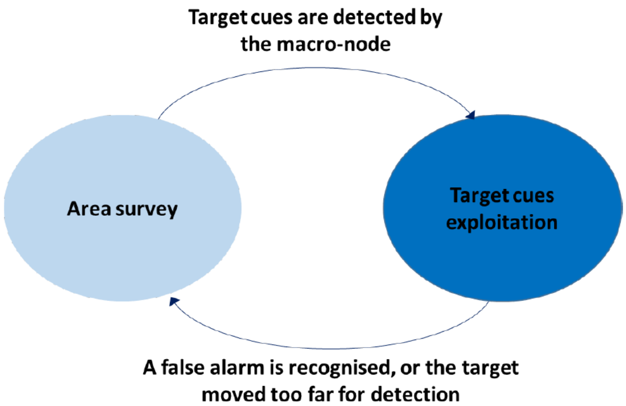

Figure 4: Mission phases for a multi-robot, persistent, passive monitoring network. In the area survey phase, the wave-gliders cooperate to achieve some coverage objectives on the area of interest. When some cues about the target are produced by the signal processing, they start to control cooperatively their navigation to confirm the target presence and to estimate its position.

In our system, we are pushing the glider autonomy to a higher level. The vehicles do not react with pre-defined behaviours, but they use data-driven strategies adapting their navigation as new information is produced. This level of autonomy is rare for a glider and can be enabled only by an accurate navigation, uncommon for typical glider navigation systems.

A high-level scheme of the robot cooperative autonomy framework is shown in Figure 5. An Occupancy Grid (OG) Mapping framework [1],[2] constitutes the perception layer. It produces maps of the probability of presence of a target in an area of interest. The produced maps are the basis for the decision layer that is in charge of cooperative decisions for fulfilling the mission objectives. The two layers are described below in more details. The interested reader is referred to [1] for further details and extensive simulation results.

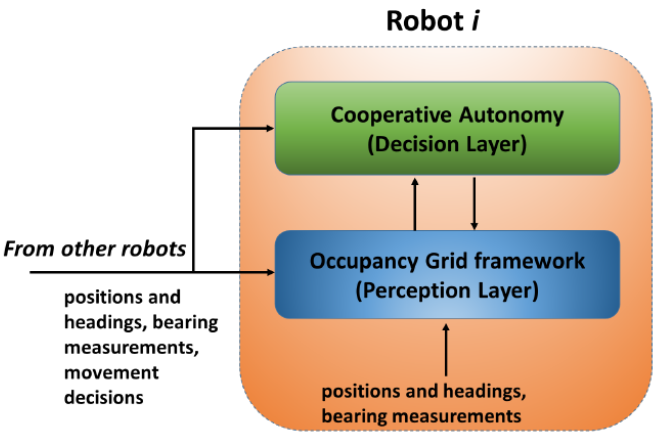

Figure 5: High-level scheme of the surface autonomous vehicle cooperative autonomy framework. An Occupancy Grid Mapping framework constitutes the perception layer, producing maps of the probability of presence of a target in an area of interest. The produced maps are the basis for cooperative decision-making.

3.1.1 The Perception Layer - OG framework

Occupancy grids were developed in 1980s as a finite-dimensional means of representing uncertainty in a robot's environment [3]. The method requires discretisation of the environment into a collection of small cells, each of which is considered as being either completely occupied or completely empty. OG mapping is the process of fusing successive noisy and uncertain measurements into estimates of the likelihood of each cell being either occupied or empty. The approach has been applied to many robotic applications. It was first used to map indoor environments [4], and, more recently, it has been adopted to map outdoor ones, such as urban areas [5].

In our application, we apply occupancy grids to map the presence of targets in an area. The binary state of grid cells is redefined to denote the probability of target presence or absence. A defining characteristic of our application considered within the context of OG mapping is the small number of cells expected to be occupied by targets (or detectable objects, such as passing vessels). This implies that the prior probability of occupancy associated with each cell is much lower than is typical in OG maps of, for instance, the layout of a building constructed from laser or sonar range-finder data [4]. In this situation, the well-known conflicts generated by standard grid mapping algorithm [4] appear to be amplified [6]. These conflicts are caused by the sensor cone that sweeps on multiple cells inducing dependencies among the cells that cannot be taken into account by the standard OG mapping algorithm [4] that estimates independently the state of each cell. A similar scenario from a prior perspective is the mapping and localisation of chemical sources [6][7][8]. In these papers the authors propose a map update rule that, in a low prior scenario, has been demonstrated to produce better maps than the standard Bayesian update rule. In particular, the resulting maps are more consistent with the true number of occupied cells, and less sensitive to the correct choice of prior. In our application we use a map update rule adapted from these works. On the other hand, our application is different from chemical sources mapping. The big difference is that targets, differently from chemical sources, move. Traditional OG mapping techniques rely on the assumption of a static world that is the mapped environment does not change over time. For this reason, an extension of OG mapping to dynamic environments will be used by applying the transition matrix of a Markov Chain (MC) [4] [10] to rule the dynamics of the probabilities of each grid cell.

Finally, it is important to underline that the used approach does not make assumptions on the presence of a single target in the area, and does not suffer from the difficulties raised by data association, usually present in tracking approaches [9].

Let C be the number of cells in an OG map. $m_{1:C}$ denotes the collection of all binary cell states and $z_{1:t}$ denotes the collection of all measurements. Then, considered as a Bayesian C-dimensional binary estimation problem, all information about the state of the map would be contained in the posterior $p(m_{1:C}|z_{1:t})$. Unfortunately, the number of possible maps is 2^C, and so it is usually prohibitive to store or compute this full posterior. Consequently, OG mapping methods typically seek the marginal posteriors for the occupancy of each cell $p(m_i|z_{1:t})$, with i=1,…C.

However, it is not possible to compute these marginals exactly without first computing the full posterior and then marginalising. To avoid the computational burden implied by this task, traditional OG mapping methods employ map update rules that attempt to generate the marginal posteriors directly from measurements and the current state of the map. The standard Bayesian map update rule produces inexact marginal posteriors, but it is simple to implement and popular [4]. For numerical reasons, the standard algorithm computes the so-called log odds of occupancy for each cell at each time step. Log odds for cell i at time t is:

$$l_{t,i} = \log \frac{p(m_i|z_{1:t})}{1-p(m_i|z_{1:t})}$$

from which it is trivial to recover the associated marginal posterior. At time $t = 0$, this quantity is initialised to the log odds prior for each cell:

$$l_0 = \log \frac{p(m_i)}{1-p(m_i)}$$

Besides the prior probability of occupancy $p(m_i)$ for each cell, the only other quantity required is an inverse sensor model to provide the probability that the cell being updated is occupied given the current measurement, that is $p(m_{ij}|z_t)$. These quantities can be used by the standard Bayesian map update, a version of the binary Bayes filter [23].

A critical assumption required in the derivation of the standard Bayesian map update is:

$$p(z_t|z_1,\ldots,z_{t-1},m_i) = p(z_t|m_i)$$

This equation states that the current measurement is independent of all other measurements predicated on knowledge of the cell currently being updated. Because sensors sweep over multiple cells, this assumption is usually incorrect and consequently the marginal posteriors computed by the standard algorithm are inexact. However, the assumption greatly simplifies the problem of computing the marginal posteriors by enabling the mapping problem to be treated as a collection of C independent binary estimation problems [4].

In order to fully specify the OG algorithm for the perception layer, it remains to define a sensor model suited to our scenario and how to handle the dynamic of a target. As mentioned above, the dynamic of the OG is ruled according to a MC model by specifying a state transition probability, $p(m_{t,i}|m_{t-1,i})$, which rules how the occupancy state of a cell m_i evolves between consecutive time steps. We assume that the modifications in the environment are caused by a stationary process *i.e.* the transition model is independent of time. The sensor model can be specified by assuming a model for the probability of detection. A full definition of both the sensor model and the dynamic model of the OG algorithm is beyond the scope of this report. The reader can refer to [2] for a detailed mathematical formulation of the entire algorithm.

Finally, the OG-based algorithm to iteratively produce a map of target position probabilities consists of two steps (see Figure 6):

- Time update (propagation).
- Measurement update.

The algorithm is activated periodically, for instance every time new measurements are available. First, the map is updated according to the MC. In particular, the MC transition model is applied to each cell of the OG map, $l_{\{t-1,i\}}$, at time t-1, where i is the index of the spatial grid cell. The produced map, $l^{-}_{\{t-1,i\}}$, is fed, together with the measurements (if any) to the Independence of Posteriors (IP) algorithm [2] to compute the OG map, $l_{\{t,i\}}$, at time t.

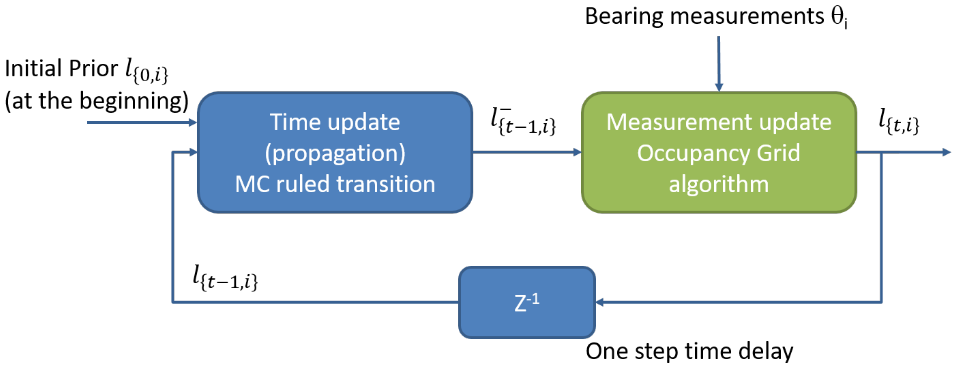

Figure 6: The proposed OG based algorithm to create a map of the target presence probability. The algorithm consists of two steps: the time update in which a MC rules the temporal transition of the cell occupancies, and the IP OG algorithm, that iteratively integrates bearing measurements produced by sensors on-board the underwater robots.

3.1.2 Decision Layer – Cooperative autonomy

The objective of area survey/patrolling is to cover with sensor measurements an area of interest. We have to quantify how well regions have been monitored and if some interesting cues likely related to a target have been encountered. We have to remark that in our case a dynamic world is considered. Therefore, an area has to be adequately surveyed again after some time from the first coverage. The produced OG maps provide a guidance for this process. They show regions interesting to be investigated more (higher target presence probability), regions likely empty and areas not adequately monitored. Furthermore, the MC dynamic model of the map, described above, provides a way to insert in the survey process some temporal constraints. If an area is not monitored for some time, the system will bring back the occupancy probability to the prior, showing that region has to be surveyed again.

One objective to drive the robot survey is the reduction of uncertainty in the produced maps. Given an occupancy grid, the entropy of each cell can be used to quantify its uncertainty. Let us denote the i-th cell by m_i, and its occupancy probability $p_i = p(m_i)$. Then the entropy of the binary occupancy variable is given by:

$$H_p(m_i) = -p_i \log p_i - (1-p_i)\log(1-p_i)$$

$H_p(m_i)$ is maximum when the occupancy is 0.5, while becomes 0 when $p_i = 0$ or $p_i = 1$, that is the cell occupancy is certain. The total entropy of the map is therefore:

$$H_p(\mathbf{m}) = \sum_i H_p(m_i)$$

The computed entropy can be the guidance for the robot navigation (see [11]). The robots survey an area moving on pre-fixed rectangular paths (called racetracks). The area survey proceeds until some cells of the map reach entropy values higher than a pre-fixed threshold. The robots then enter the target cues exploitation phase and cooperate for localising the target.

In the following, we will consider two robots that produce bearing-only measurements and move at constant speed. The cooperative target localisation behaviour controls the robot heading angles with the objective of optimising the estimate of the target x-y position through data fusion between maps produced by different assets. The behaviour has a distributed nature. Each robot makes a decision evaluating the current navigation decision and map of the collaborator. The cooperative robot decisions drive the sensors towards spatial configurations favourable for achieving target localisation. The achieved configurations are beneficial not only from a geometric perspective, but also from the point of view of sensor probability of detection. A trade-off is found between these two objectives that may be conflicting. Data fusion between the measurements produced by different assets is central. For these reasons, communication has to be guaranteed and constraints in the robot navigation has to be inserted, together with redundancy communication policies to tackle the unavoidable packet loss.

Looking at the literature, several approaches for bearing-only measurements such as Target Motion Analysis have been proposed for target localisation [12]. However, most for them rely on the hypothesis of straight and constant-speed motion of the target. Furthermore, a single robot would need speed higher or comparable with that of the target. This would allow it to manoeuvre for detecting the target at diverse bearing angles. In order to relax these constraints, the most robust approach is to fuse the Direction Of Arrival (DOA) results from at least two platforms in the network, using for instance information-theoretic distributed control strategies [13][14][15].

The OG perception layer can support this approach, and data fusion from different sensors can compensate for robot limited speed.

Maps produced by robots can be used to estimate the target position and offer a way to plan cooperative actions. Let us define the map produced by the robot 1 at time t as $p_1(\mathbf{m})$, and the map produced by the robot 2 as $p_2(\mathbf{m})$, where $\mathbf{m}=[m_1,,m_C]$. We assume that the robots exchange measurements and their position/heading, so each vehicle has access to the information necessary to compute both maps. The fused map can be computed multiplying the occupancy of each corresponding cell, that is for cell i, $p_f(m_i) = p_1(m_i)p_2(m_i)$.

We have now to identify one effective metric to quantify the target localisation. For accurate target localisation, we aim at having one cell with high occupancy probability, surrounded by cells with low occupancy probability. One possible solution to quantify this is to compute the Laplacian of the fused occupancy map, $p_f(\mathbf{m})$, that is $LP_f(\mathbf{m})=\nabla^2[p_f(\mathbf{m})]$. For each cell i a value of the Laplacian is therefore produced, $LP_f(m_i)$. In mathematics, the Laplace operator or Laplacian is a differential operator given by the divergence of the gradient of a function on an Euclidean space. If we consider $p_f(\mathbf{m})$ as a scalar field, cells with large negative values of $LP_f(m_i)$ are characterised both by high occupancy probability and are surrounded by low occupancy probability cells. These cells are peaks in the probability map. This is exactly what we are searching for. The map $LP_f(\mathbf{m})$ is therefore used as a good indicator of the target position.

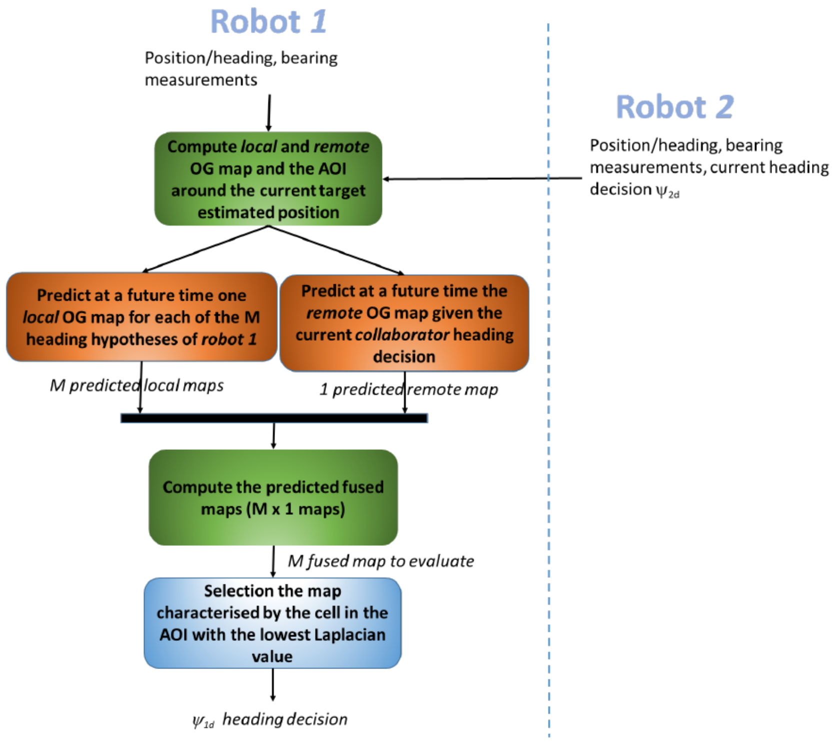

Figure 7: Cooperative and distributed selection of heading decision for target localisation - actions performed by robot 1. The robot 1 computes the local OG map and the remote one using the data received from robot 2. Then it predicts at a future time the state of the local OG map following M heading hypothetical decisions. Robot 1 also predicts at a future time the remote OG map resulting from the collaborator's decision. Then, it creates M predicted fused maps and for each map computes the Laplacian of the cells. The map containing the cell in the AOI with the lowest Laplacian value is selected. The relative heading decision, ψ_{1d}, is selected as command until the next decision time and transmitted to the collaborator.

The robot control algorithm seeks for wave-glider heading angles that create favourable $LP_f(\mathbf{m})$ maps. The algorithm steps are shown in Figure 7. The figure reports for simplicity the actions that robot 1 executes to produce its desired heading, ψ_{1d}, at a certain decision time.

The robots exchange their position/heading, the produced bearing measurements and their current heading decision ψ_{1d} (for robot i). At a certain decision time, one robot, let us say robot 1 for simplicity, performs the following steps:

- Compute an Area of Interest (AOI) W around the cell that contains the current estimate of the target position.
- For the remote robot, robot 1 predicts the following map:

$$E'_{z2}(\mathbf{m}) = E_z[p_2(\mathbf{m}|\mathbf{z}, u_2)]$$

  with E'_z being the expectation operator with respect to measurements $\mathbf{z}$. The superscript indicates that the map is predicted in the future following an action of the robot. The robot computes a prediction map at a future time averaging over the possible measurements $\mathbf{z}$ that robot 2 could collect at its predicted future position/heading given its action, u_2. In this case, u_2 is the action (movement and rotation) caused by the current robot 2 heading decision, ψ_{2d}, for a certain prediction time.
- For robot 1, M possible heading decisions $\{\psi_{11}, \psi_{12,}, \psi_{1M}\}$ are selected around the current heading angle. For each of these movement hypotheses, ψ_{1i}, a predicted map at a future time is computed as described in the previous step. Specifically, for the action ψ_{1i}:

$$E'_{z1i}(\mathbf{m}) = E_z[p_1(\mathbf{m}|\mathbf{z}, u_{1i})]$$

  The map E'_{z1i} is created from the local OG map and the possible measurements collected by robot 1 at the predicted future position/heading given the action u_{1i}. A total of M maps is computed in this way, one for each possible heading decision.
- Then, for each of the heading action of robot 1, we compute:

$$LP'_f(\mathbf{m}|u_{1i}, u_2) = \nabla^2[E'_{z1i} \cdot E'_{z2}]$$

  Where the operator $\cdot$ is intended as a multiplication cell by cell of the two resulting maps. The Laplacian operator is applied to the resulting expected fused map, following the vehicle actions.
- Finally, we select the action u_{1d} that produces the map that, inside its AOI, contains the cell with the lowest Laplacian value. That is:

$$u_{1d} = \arg\min_{u_{1i}} LP'_f(m'_i|u_{1i}, u_2), |m_i \in \Omega$$

The computation of the quantities E'_z=$E_z[p(\mathbf{m}|\mathbf{z},u)]$ is in general not trivial, since all possible measurements following an action u should be evaluated. One way to approximate the computation is via the so-called “hallucinated” measurements that are usually computed via approximate ray-casting techniques in conjunction with a plausible sensor model. The reader can refer to [16] for a detailed introduction to the method.

During target localisation, the robots need to satisfy some cooperative navigation constraints. It is necessary to guarantee communication connectivity (maximum inter-vehicle distances), as well as avoid collisions between robots (minimum inter-vehicle distances). A task priority (TP) framework has been developed for introducing this kind of geometrical constraints in the team control laws. If we assume to have tasks with different degrees of priority, TP control allows the execution of the lower priority tasks without affecting the execution of the higher priority ones. In our case, we identify three different prioritised tasks: collision-avoidance, reach a location and keep the connectivity. We build the desired team behaviour dynamically modifying the priorities of the mission tasks. The robots cooperatively reach a desired geometric localisation, at the same time guaranteeing a limited inter-node distance and avoiding possible collisions.

3.1.3 Preliminary evaluation of component KPIs

A sea trial has been organized and executed in the Ligurian Sea to test the PERSEUS sensor array. During the test trial, a rubber boat has been used as test target with a GPS on board to acquire position and angle of arrival ground truth data. The target performed a series of test trajectories at constant speed and constant range as depicted in Figure 8 on the left.

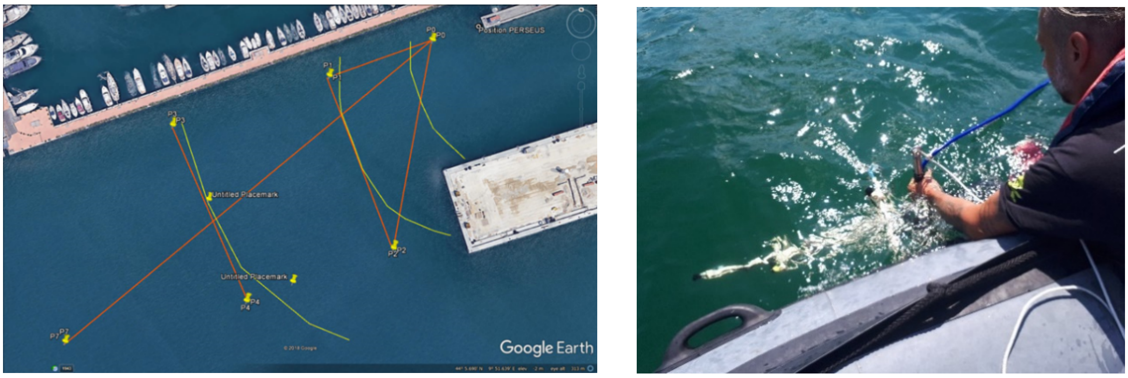

Figure 8: The experiment setup to test the PERSEUS array. On the left, in red the constant speed test target trajectories while in yellow the constant range ones. On the right, the deployment of the PERSEUS array

The test consists in acquiring data to check the capability of the sensor to detect surface targets and to understand the extent of the error on the target direction of arrival estimation which impacts the cooperative localization algorithm detailed above. Figure 9 shows an example of the signals acquired by the 8 hydrophones of the PERSEUS array while Figure 10 shows an example of the spectrogram of the signal from one of the hydrophones.

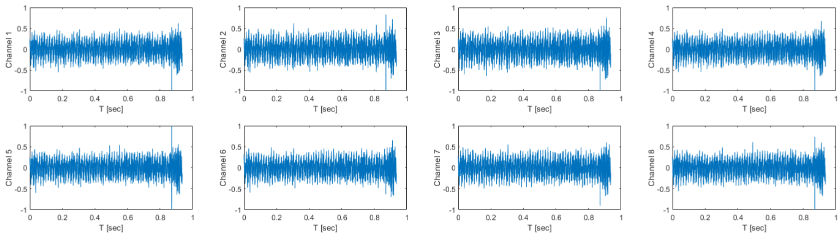

Figure 9: Example of signals acquired by the 8 hydrophones forming the PERSEUS array.

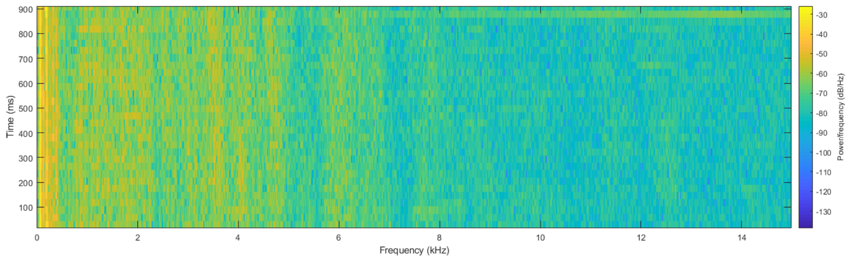

Figure 10: Example of time-frequency spectrogram analysis of the signal from one of the hydrophones of the PERSEUS array.

The 8 signals have been processed and beam-formed to automatically detect the test target and estimate the target direction of arrival. Figure 11 shows, in red, the estimates of the direction of arrival of the detected contacts in a time window of about 200 sec. The agreement with the ground-truth from the GPS in blue is quite good. Residual errors will be reduced by fusing angle measurements from different sensors using the cooperative localization approach detailed above. The data acquired during the test trial will be further processed to provide quantitative error estimates under different target trajectories.

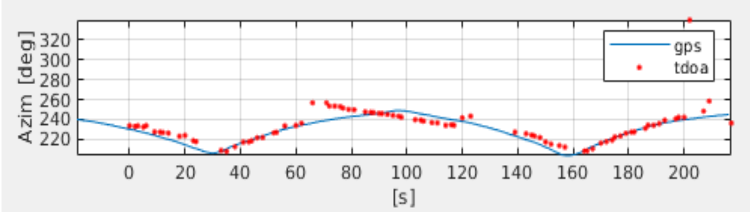

Figure 11: Target direction of arrival estimation (in red) compared with ground-truth target direction data from the on-board GPS.

The target localization algorithm was investigated through Matlab (©MathWorks) simulations. The aim was to assess the utility of the data-driven approach with respect to traditional pre-fixed paths. Furthermore, the data-driven algorithm performance was evaluated considering different target motions and different measurement qualities (perfect vs. realistic bearing measurements).

We use an area of 5 x 2 km in all the described simulation results. Two robots are used, robot 1 and robot 2. The robots move with a constant speed of 1.5 m/s. The robots exchange every 5s (at each Update Time, UT) their position/heading, heading decision, other data relative to the cooperative behaviour (state and next UT of activation) and bearing measurements. Perfect communications are assumed.

We consider the figure (a) of Figure 12 as an example of all the presented pictures. Robot 1 position is described with a black circle and the current heading with a segment originating from the robot location. The sensor footprint is shown as two black lines that delimit the sensor footprint. The sensor endfire is located at front/back of the robot. The black circles of different size in front of the robot are the decisions evaluated in the target localization behaviour. The size is relative to the value of the minimum Laplacian of the expected fused map. The selected decision is marked with a larger black hollow circle. Bearing measurements of the real target are indicated by a black cross, while triangles indicate bearing measurements due to false alarms. The same quantities are indicated in red for robot 2. The number between the robot is their distance in meters. A green diamond indicates the target, while a green asterisk shows the estimated target position (at the current UT) for robot 1. The black asterisk shows the estimated target position used during the previous step of the decision making. The black and green asterisk positions may or may not coincide.

In the scenario of Figure 12 the target starts at location (2550;550) and then moves at a speed of 2 m/s along a rotated square with a side length of 400 m and with the first waypoint position at (2450;650) (as shown in (a) of Fig. 23). In Figure 12 we report the Laplacian LP of the map produced by the fusion of single robot maps in the case of two robots moving along horizontal rectangular patterns (named racetracks) 550 m long, with robot 1 moving westwards and robot 2 eastwards at different. We show the situation at different UTs: 20, 40, 50, 110. The initial inter-robot distance is 450 m. Realistic measurements are used. As can be seen in the figures, the robots are able to localise the target at the beginning of the run. Then, the target moves north-west making the detections by robot 2 that is navigating eastwards more complex. The target following movement along the north-east leg makes it hardly detectable since the range from the robots increases.

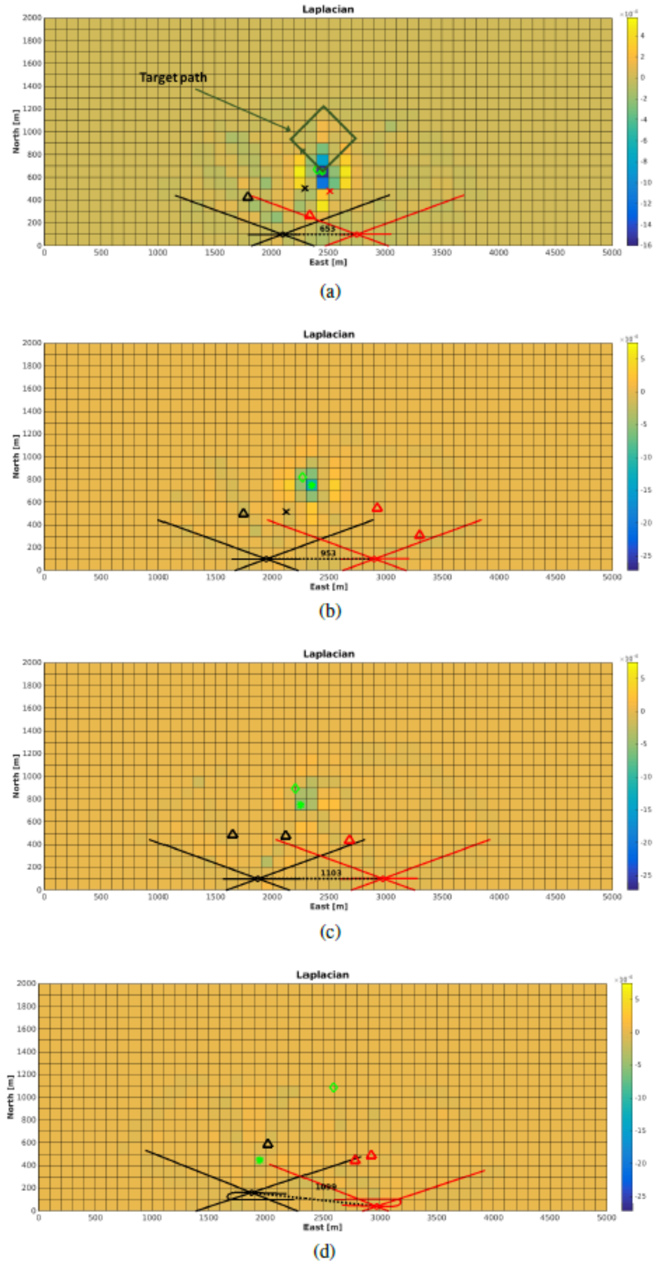

Figure 12: Target moving, robots covering horizontal racetracks, realistic measurements. UT =20 (a), UT=40 (b), UT =50 (c), UT =110 (d): Laplacian LP of the map produced by fusing the single robot maps.

The same quantity is shown in Figure 13 for simulations with the data-driven target localisation that control the robots and realistic measurements. At UT = 40 the target enters the sensor end-fire of robot 1 (see (b)). Robot 1 avoids this situation deciding to turn north-west (see (c)). Then, similarly to the perfect measurements case, turns eastwards to get closer to the target. Robot 2 in both cases behaves similarly. Overall, it moves northwards and supports the actions of robot 1 for producing favourable geometries for target localisation.

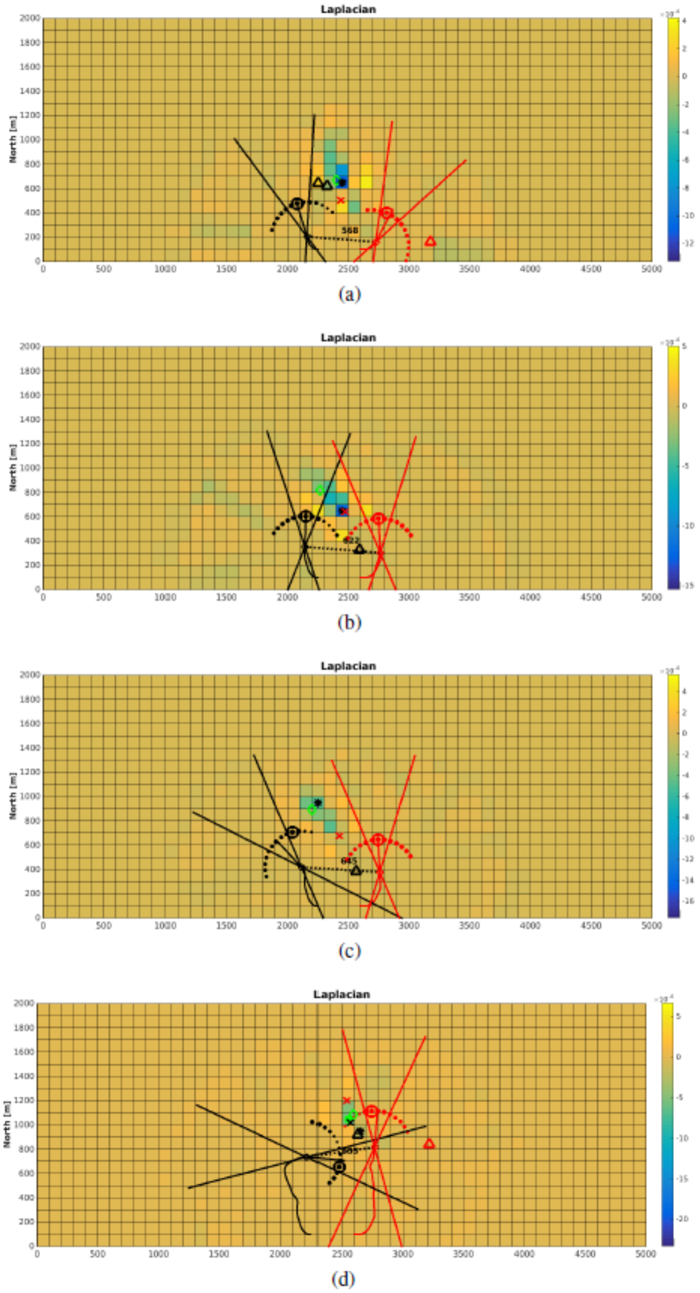

Figure 13: Target moving, robots controlled by the data-driven algorithm, realistic measurements. UT = 20 (a), UT = 40 (b), UT = 50 (c), UT = 110 (d): Laplacian LP of the map produced by fusing the single robot maps.

In Fig. 26 we report the target position estimate error and the P_d of simulations with the robots following the horizontal racetracks and controlled by the data-driven algorithm, both with realistic measurements. From the figure, it is clear how the cooperative behaviour is crucial for achieving target localisation with a target following a complex path. After time t = 300 both the robots in the racetrack case are no more capable of detecting the target. Only the robot autonomy allows them to follow and localise the target.

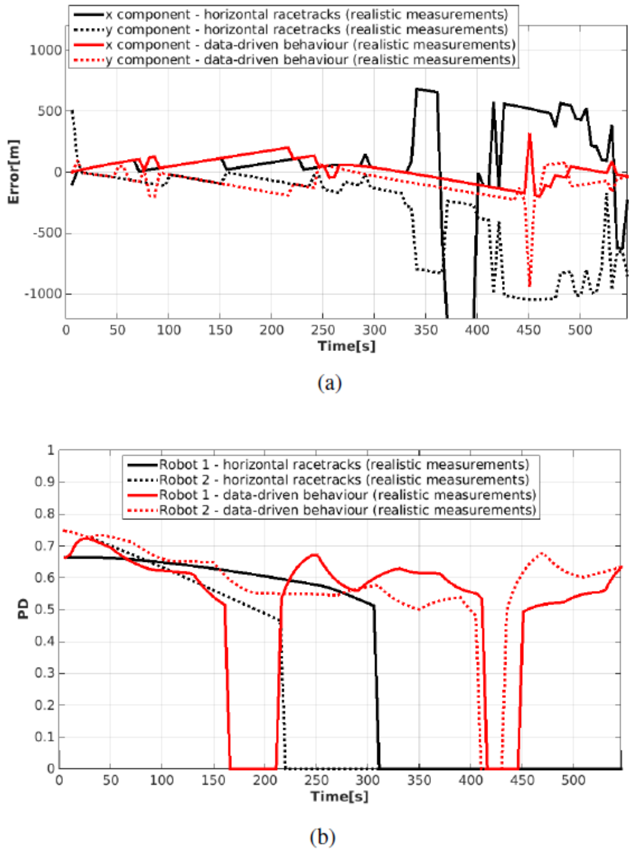

Figure 14: Realistic measurements. Target position estimate error (a), Pd at target location (b) for robots covering horizontal racetracks and controlled by the cooperative target localisation behaviour.

3.2 Target detection and classification from thermal/video camera data

In this section we describe a preliminary version of the object detection algorithms in photos and videos of vessels. Due to the COVID-19 situation, the thermal camera has not been accessible to the time of writing this document, so we decided to use simulated data in order to test approaches for performing object detection in camera data. Due to the fact that camera data are very different (in terms of format, resolution and information stored) from satellite and acoustic data, different approach should be followed for object detection in each approach.

The data that we used instead of thermal camera data were vessel photos acquired from the MarineTraffic website[1]. MarineTraffic has a large repository of photos uploaded by enthusiasts and professionals of in the Maritime domain and this repository is one of the most popular features of the MarineTraffic website.

3.2.1 Goal

The goal is to be able to identify and locate vessels (and possibly other objects as well) in photos/videos[2]. In other words, the goal is to perform object detection and segmentation.

Another motivation for this work is the fact that in this way, we will be able to identify photos that are erroneously annotated as vessel photos in the MarineTraffic website.

[1] https://www.marinetraffic.com/en/photos/of/ships

[2] Since videos are composed of frames, we handle videos and photos uniformly.

3.2.2 Solution

Core part of the solution is to use Convolutional Neural Networks (CNN). But unlike the task of vessel detection in satellite imagery, where the resolution is low, the vessels appear as small objects, and the number of different objects located in each tile is very low, the case in data coming from cameras is different. The fact that the resolution in this case is higher, combined with the fact that cameras are usually located in places where other activities also take place (e.g., ports, terminals, beaches, etc.) introduces more challenges: The vessels appear bigger with the vessel shape and portrayed dimensions varying according to the height and angle of the camera the photo is taken, while many other objects (e.g., people, port/terminal facilities, buildings, etc.) might also appear in the same photo or even tile. To make things worse, the MarineTraffic photos were taken using different cameras and of course, different angles for each vessel. So, given these differences, the CNN architectures employed for the vessel classification tasks for satellite data, another CNN architecture should be employed for this dataset.

	Type	Filters	Size	Output
	Convolutional	32	3 × 3	256 × 256
	Convolutional	64	3 × 3 / 2	128 × 128
1×	Convolutional	32	1 × 1	
	Convolutional	64	3 × 3	
	Residual			128 × 128
	Convolutional	128	3 × 3 / 2	64 × 64
2×	Convolutional	64	1 × 1	
	Convolutional	128	3 × 3	
	Residual			64 × 64
	Convolutional	256	3 × 3 / 2	32 × 32
8×	Convolutional	128	1 × 1	
	Convolutional	256	3 × 3	
	Residual			32 × 32
	Convolutional	512	3 × 3 / 2	16 × 16
8×	Convolutional	256	1 × 1	
	Convolutional	512	3 × 3	
	Residual			16 × 16
	Convolutional	1024	3 × 3 / 2	8 × 8
4×	Convolutional	512	1 × 1	
	Convolutional	1024	3 × 3	
	Residual			8 × 8
	Avgpool		Global	
	Connected		1000	
	Softmax			

Figure 15: Darknet-53 layered architecture. The table provides, for each layer, the type of layer, the number of convolutional filters, the size of the filter window in pixels and the size of the output grid.

We used the You Only Look Once (YOLOv3) framework that relies on Darknet, an open-source c-based Neural Network framework[3]. YOLO [35] is a state-of-the-art framework that employs CNNs for object detection and segmentation. We used its latest version (v3) that is able to outperform well-known CNNs both in terms of accuracy and performance[4]. For example, it outperforms older variations of Darknet (Darknet-19) and ResNet [47]. YOLO extends the Darknet-19 architecture with additional layers. The new neural network architecture is called Darknet-53 due to its 53 layers, shown in Figure 15.

For training, we used the well-known COCO dataset[5] [36] for the following reasons:

(a) It is a large, well-known, well-maintained dataset produced by Microsoft, with contributions from Google and Facebook.

[3] https://pjreddie.com/darknet/

[4] https://pjreddie.com/darknet/yolo/

[5] T.-Y. Lin, M. Maire, S. Belongie, J. Hays, P. Perona, D. Ramanan, P. Dollar, and C. L. Zitnick. Microsoft coco: Com- ´ mon objects in context. In European conference on computer vision, pages 740–755. Springer, 2014.

(b) It includes more than 80 classes, with more than 3000 images from vessels that are very similar to MarineTraffic vessel photos.
(c) It is suitable for image segmentation, as images are annotated with the bounding boxes of the identified objects.
(d) Due to the fact that the COCO dataset includes a lot of instances of over 80 classes, it will help as identify additional objects in photos apart from vessels.

3.2.3 Preliminary evaluation

We performed preliminary evaluation using a Python-based implementation of the YOLO v3 framework trained on the COCO dataset (we used pre-trained weights) and 1000 completely unseen MarineTraffic images, with and without vessels.

The accuracy achieved was 79%. In the next round of experiments this accuracy is expected to be increased by annotating MarineTraffic photos that were false positives in the first round of experiments, and including them in the training set, while testing against new, unseen MarineTraffic photos. The new round of experiments will be executed in the BSC cluster in order to exploit the GPU capabilities.

Figure 16: Output of the first round of experiments on MarineTraffic unseen imagery performing multi-class identification (e.g., instances of classes "person" and "boat").

Figure 17: Another MarineTraffic image annotated with the output of the classification task, i.e., identifying and locating vessels (e.g., instances of the class "boat").

4 Global view sensors

This work makes use of data from two sources: the AIS and the Sentinel 2 Multi-spectral instrument (MSI) sensor. Data from the two systems are fused to automatically extract training data sets by using the procedure detailed below.

4.1 The AIS

The Automatic Identification System (AIS) [31] is an automated, autonomous tracking system which is extensively used in the maritime world for the exchange of navigational information between AIS-equipped terminals. Thanks to it, static and dynamic vessel information can be electronically exchanged between AIS-receiving stations (onboard, ashore or satellite).

Since December 2004, the International Maritime Organisation (IMO) requires all passengers' vessels, as well as, all commercial vessels over 299 Gross Tonnage (GT) that travel internationally to carry a Class A AIS transponder (which transmits and receives AIS data) aboard (smaller vessels can also be equipped with a Class B AIS transponder). This decision came as a result of the 2002 SOLAS (Safety of Life at Sea) agreement's relative mandate.

AIS transponders (on vessel stations) include a GPS (Global Positioning System) receiver which collects the subject vessel's position and movement details. Such (dynamic) details along with other static information provided by the vessel's crew are automatically broadcasted at regular intervals via a built-in VHF transmitter using 2 specific VHF channels (161.975 Mhz and 162.025 Mhz - 87 & 88 old VHF channels).

The periodic AIS-data information can be received by other vessel or base stations (provided they are within range). Then, with the use of special software, it can be processed and depicted on chart plotters or on computers (for example, on the MarineTraffic Live Map). AIS-data can also be received by satellites - in this case, the term Sat-AIS is used (Satellite AIS or S-AIS).

The availability of the AIS information to the public domain quickly led to a drastic change regarding the initial perception of its use. AIS was originally developed by IMO (International Maritime Organisation) as a standard which would help vessels to avoid collisions while assisting port authorities to control marine traffic with more efficiency.

4.1.1 AIS Issues

Despite the widespread use of AIS and its contribution in raising the maritime awareness and safety of navigation, it comes with the following issues:

1. Ship identification is challenging sometimes. The most secure way to uniquely identify a vessel is each IMO number, which is unique and mandatory for all cargo vessels that are at least 300 Gross Tons (GT) and passenger vessels of at least 100 GT according to SOLAS regulation XI/3. However, not all vessels fall into these categories, thus, they do not have an IMO number. Another characteristic that can be used to identify vessels is the MMSI, which is a number that consists of 9 digits and it is mandatory for all vessels. As this number can be modified under certain conditions, although is it not very usual for multiple vessels to have the same MMSI, it cannot be considered as a unique identifier.
2. Part of the information transmitted in AIS messages is completed manually by the vessel's crew. This means that the AIS data might occasionally be prone to errors, noisy, inconsistent, and fields might be inaccurate or completely missing because of human error.
3. Equipment Malfunctions. Transponder malfunctions might happen, leading to vessels not being able to transmit messages at all, or not in the rate they are obliged to (e.g., more frequently when they are under way with high speed).
4. Intentional switch-off of the AIS transponder. Lately, the phenomenon of intentional switching off the AIS transponders by the crew becomes more usual than before (e.g., due to recent sanctions applied, etc.). This could happen for example when a vessel is about to engage in illegal activities (e.g., smuggling, illegal fishing, entering a protected zone, etc.).

Due to the issues described above, although AIS is a significant source of information about the Maritime Situational Awareness, in order to obtain a complete picture of the maritime domain, it should be combined with additional sources of information, such as satellite images, acoustic data, data from thermal cameras, etc. One of the objectives of this use case is to perform fusion of AIS data with additional, heterogeneous sources, as described in the following sections.

4.2 Sentinel 2 multi-spectral instrument sensor and data

The MSI is a push broom multi-spectral passive imaging sensor on board the European Space Agency (ESA) Sentinel 2 satellite constellation used for Earth observation [32]. The constellation consists of two polar orbiting satellites, 2A and 2B, placed on the same orbit and phased at 180° to each other. The revisit time with two satellites is 10 days at the equator and 2 to 3 days at mid-latitude. The latitude coverage is between 56°S and 84°N and the swath width is 290Km. The MSI sensor acquires the solar radiation from the Earth surface and the atmosphere in 13 spectral bands, four bands at spatial resolution ΔR=10m, six bands at ΔR=20m and three bands at ΔR=60m, with a radiometric resolution of 12bits. The channels at ΔR=10m are the most interesting ones for ship classification. Table 3 shows the characteristics of these channels for the MSI on board Sentinel 2A and 2B [33], including the central wavelength, λ_0, the spectral resolution, Δλ, the calibration reference radiance, L_{ref}, and the signal to noise ratio at the reference radiance, SNR@L_{ref}. The first 3 channels cover the visible spectrum in the blue, green and red bands, respectively, while the fourth channel covers a band in the near infrared (NIR) range. The data at 10m resolution are provided as image tiles (or granules) on a geo-located uniform grid of 10800 by 10800 samples for each spectral channel and are freely available through the Copernicus Science Hub (CSH) web site [34].

Table 3: Sentinel 2 MSI sensor characteristics.

Band number	S2A		S2B		L_{ref} $(Wm^{-2}sr^{-1}\mu m^{-1})$	$SNR@L_{ref}$
	$\lambda_0(nm)$	$\Delta\lambda(nm)$	$\lambda_0(nm)$	$\Delta\lambda(nm)$		
2	492.4	98	492.1	98	128	154
3	559.8	45	559	46	128	168
4	664.6	38	664.9	39	108	142
8	832.8	145	832.9	133	103	174

Sentinel 2 MSI data are mainly used to identify vessels that might have their AIS transponders switched off or that are transmitting false AIS information like a wrong ship type. To this purpose, a set of machine learning classifiers are designed to estimate some attributes of a ship target given the target spectral signature acquired by the sensor. The information provided by a classifier is then compared with the context information provided by the AIS contacts in the area of interest and anomaly are detected if the two information are not coherent. The next sub-sections describe the classifiers and provides evaluation of the classification performance. Figure 18 shows an example of ship target spectral signatures for a Moss-spherical liquid natural gas (LNG) tanker from which is possible to see several features characterizing the target.

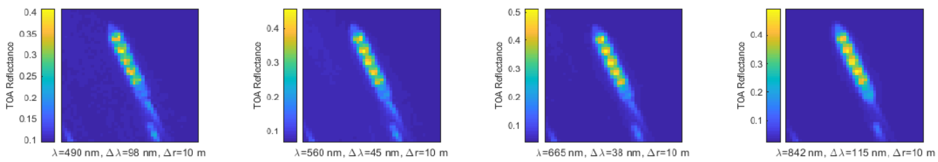

Figure 18: Example of an MSI spectral ship target signature for a LNG Moss-Spherical tanker.

4.2.1 Convolutional neural network classifiers

The architecture of the classifiers used in the project is based on deep convolutional neural networks [17]. Figure 19 shows the neural network used in this work to build the ship target classifiers. In general, the network can process input data coming from *M* different sources, or modalities, and integrate information at the feature level by means of a combination layer. Each branch of the system has a multilayer convolutional block followed by a dense layer entering the combination layer. Dropout layers can be added to regularize the network. The combination layer is followed by a multi-layered fully connected sub-net with *K* outputs, where *K* is the number of target classes. These outputs provide the scores to the final max-rule layer to choose the target class having the maximum probability. A prior probability can be associated to the weights of all the layers of the network, or part of them, and the network can be trained by minimising the cross entropy loss function or using a Bayesian variational inference method by maximizing the evidence lower bound (ELBO) loss function [18].

The specific network used to classify ship targets from MSI images has two branches, one for each resolution, ΔR=10m and ΔR=20m, considered as two different acquisition modalities. The image channels having the same resolution are assigned to a branch of the network. The system structure has a high degree of flexibility and can be configured as needed by including or excluding branches, depending on the available modalities, and considering different channel combinations. In this report, the full multi-modal structure is tested, while in future work, the performance of different system configurations will be compared to evaluate the minimum number of branches and channels needed to achieve a given level of performance.

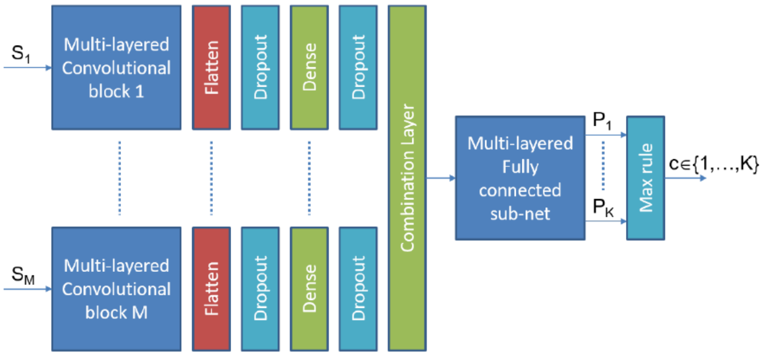

Figure 19: Multi-modal classifier based on convolutional neural networks.

4.2.2 Classifiers and training data sets

The classifiers considered in this report include a) a binary ship/no-ship low level classifier, b) a binary low-speed classifier, c) a 4 class course over ground (COG) quadrant classifier and d) a 4-class ship type classifier. An additional ship type classier with broader ship classes {"Cargo", "Tanker", "Other"} is also taken into account.

The ship/no-ship classifier is a low-level classifier that is used to discriminate between ship targets and non-ship targets like clouds. The other ones are applied afterward to understand some additional properties of the target, acquiring a rough idea of the navigational status (an information that is correlated to the presence of a ship wake) and the identity.

Specific training sets are built for each classifier by using a semi-automatic association procedure between AIS contacts and target contacts automatically detected on a set of MSI images. Once an image contact is associated to an AIS contact in a certain position and time instant, the AIS attributes of the corresponding AIS message are used to label the ship target MSI sub-image. Residual association errors are corrected by visual inspection of the produced data set.

The main training data set obtained by using the procedure above is then used to extract training examples for each of the considered classifier. Concerning the low-level classifier, 2000" no-ship" targets and 2000 "ship" targets were extracted from the main data set. Then 50% of the samples of each class were assigned to the training set, 25% to the validation set and 25% to the test set. Regarding the low speed classifier, a data set of ship targets longer than 200m was first extracted. This set was split in two classes of 1100 samples for each class by using a 1Knot threshold on the speed over ground (SOG). Finally, 70% of the samples were assigned to the training set, 15% to the validation set and the remaining 15% to the test set. For the COG quadrant classification task, 250 ship targets for each quadrant (Q1 = Northern-Eastern, Q2 = Northern-Western, Q3 = Southern-Western and Q4 = South-Eastern quadrants) were picked at random. Then 60% of the samples were assigned to the training set, 20% to the validation set and the other 20% to the test set. The data set for ship type classification was extracted by searching for targets in a given list of vessels. In particular, four groups of ships are taken into account: a) a fleet of cargo ships of a given shipping company, b) a group of liquid natural gas (LNG) tankers of the spherical Moss type, c) a fleet of roll-on/roll-off (RORO) vehicle carrier ships and d) a set of very large crude carriers (VLCC) and ultra large crude carriers (ULCC) oil tankers. Ships in each group share similar structural characteristics and spectral signatures. The size of each group is of 75, 33, 99 and 104 target images, respectively. The 30% of the targets were assigned to the training set, 35% to the validation set and the other 35% to the test set. The training set is finally augmented as described in section 4.2.3o reduce the effects of small sample over-fitting phenomena. Due to the small size of this data set the results obtained on the ship type classifier are not definitive. Further investigations will be conducted in the future by collecting additional samples. Finally, the data set for the coarser ship classifier for the classes "Cargo", "Tanker" and "Other" has a number of samples of 3066, 2071 and 1231, for each class, respectively, for a total of 6368 samples. The data set is split in 80% training set and 20% validation set.

4.2.3 Mitigation of over-fitting due to small data sets

Over-fitting due to small sample is further reduced by augmenting the training sets. The augmentation procedure consists in applying random geometric and pixel-wise value transformations to the training images to produce new samples. The image transformations include:

- random translation of a maximum amount of 3 pixels in both spatial directions,
- random spatial scaling with a scale factor between 0.8 and 1.2 on both directions,
- random rotations between 0 and 30 deg (not applied in the case of COG classifier)
- and random scaling of pixel values with a factor between 0.8 and 1.2.

4.2.4 Classifier KPIs

Binary classifier performance is evaluated by ROC curves which display the classifier true positive rate (TPR) versus the false positive rate (FPR), for several values of the decision threshold applied to the network score of the positive class. For multi-class problems the ROC curve is estimated by taking one class as positive while the remaining ones are joined in a single negative class. The classification score used to estimate the ROC curve in this case is re-computed as $m_i = p_i - \max_{j \neq i}(p_j)$, where $i, j = 1;\ldots,K$, i is the index of the chosen positive class, and p_i is the score at the output of the classifier for the i^{th} class. A bootstrap method is then used to estimate ROC curves and AUC confidence intervals allowing testing if the trained classifier statistically outperforms the TPR=FPR classifier with AUC=0.5.

4.2.5 Performance evaluation

This section shows the performance of low-level and high-level CNN classifiers, which were trained using the data sets described above. Figure 20 shows the scatter plots of the features learned by the vessel speed classifier and calculated on the training set. The features are the outputs of the dense layer just before the final layer outputting the classification scores and are indicated as F_i, where i is the output index. The degree of separation of the two classes in the learned feature space is quite good and they can be easily discriminated by a simple classification law. Figure 21 shows the same scatter plots for the features learned by the ship type classifier and calculated on the training set. Even in this case, the three classes are very well separated allowing to reach a classification accuracy of about 97% for both the training and the validation sets.

Table 4 summarizes the AUC statistics of the four main classifiers introduced above, i.e. the AUC point estimation and AUC 95% confidence intervals (CI). Figure 22-a) shows the ROC curves and the associated 95% CIs of the ship/no-ship low level classifier estimated for the training, validation and test sets. The estimated 95% CI of the AUC is (0:954; 0:986) for the validation set, (0:940; 0:976) for the test set and (0:985; 0:998) for the training set, with AUC point estimation of 0.975, 0.962 and 0.995, respectively. Figure 22-b) shows the same curves for the low speed classifier. The estimated 95% CI of the AUC is (0:914; 0:969) for the validation set, (0:940; 0:978) for the test set and (0:995; 0:999) for the training set, with AUC point estimation of 0.952, 0.962 and 0.998, respectively. The ROC curves of the 4-class COG quadrant classifier for the three data sets are displayed in Figure 22-c). The graph is relative to the Q1 class taken as positive while the remaining ones are considered as a single negative class as described in section III-D. The estimated 95% CI of the AUC in this case is (0:945; 0:996) for the validation set, (0:932; 0:992) for the test set and (0:997; 0:999) for the training set, with AUC point estimation of 0.983, 0.974 and 0.998, respectively. Similar results were obtained taking the Q2, Q3 and Q4 quadrants as positive classes. Finally, the performance of the 4-class ship-type classifier is displayed in Figure 22-d) for the ”fleet of cargo” class taken as positive. The estimated 95% CI of the AUC is (0:956; 0:996) for the validation set, (0:984; 1) for the test set and (0:994; 0:999) for the training set, with AUC point estimation of 0.986, 0.998 and 0.997, respectively. Similar performance is achieved when the other classes are considered as positive. In general, the performance of the proposed CNN structure is good with an estimated AUC greater than 0.95 in all the cases taken into account.

Table 4: Classifier performance indices. Estimation of mean AUC and confidence levels for the training, validation and test sets. Mean AUC and confidence levels are estimated using a bootstrap procedure.

	Training set	Validation set	Test set
	AUC / 95% CI	AUC / 95% CI	AUC / 95% CI
Ship/No-ship	0.995 / (0.985, 0.998)	0.975 / (0.954, 0.986)	0.962 / (0.940, 0.976)
Low speed	0.998 / (0.995, 0.999)	0.952 / (0.914, 0.969)	0.962 / (0.940, 0.978)
COG Quadrant	0.998 / (0.997, 0.999)	0.983 / (0.945, 0.996)	0.974 / (0.932, 0.992)
Ship type	0.997 / (0.994, 0.999)	0.986 / (0.956, 0.996)	0.998 / (0.984, 1)

The coarser ship type classifier, not shown in Table 4 and Figure 22 for the sake of brevity, achieves a classification accuracy greater than 95% in line with the accuracy of the other four classifiers confirming the validity of the approach used to classify ship targets.

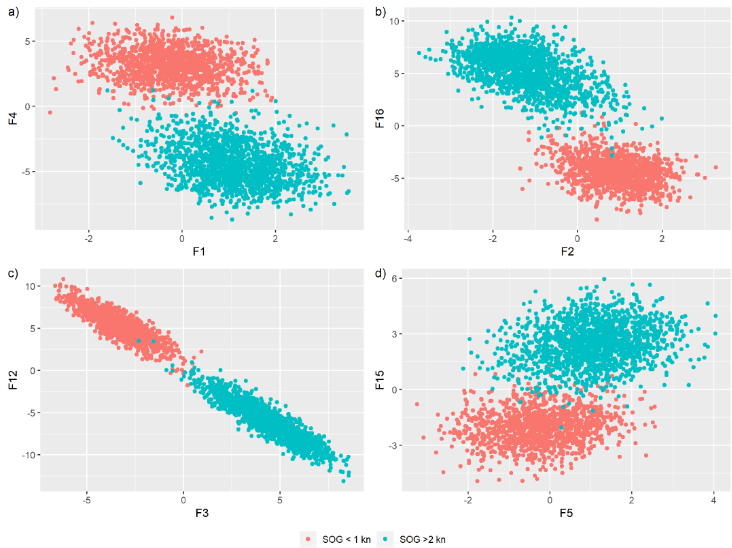

Figure 20: Ship speed classifier features.

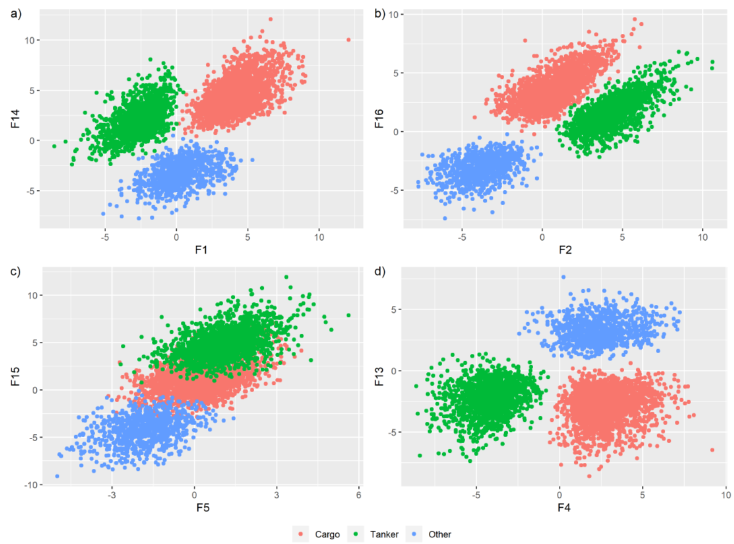

Figure 21: Feature of the ship type classifier for classes equal to {"Cargo", "Tanker", "Other"}.

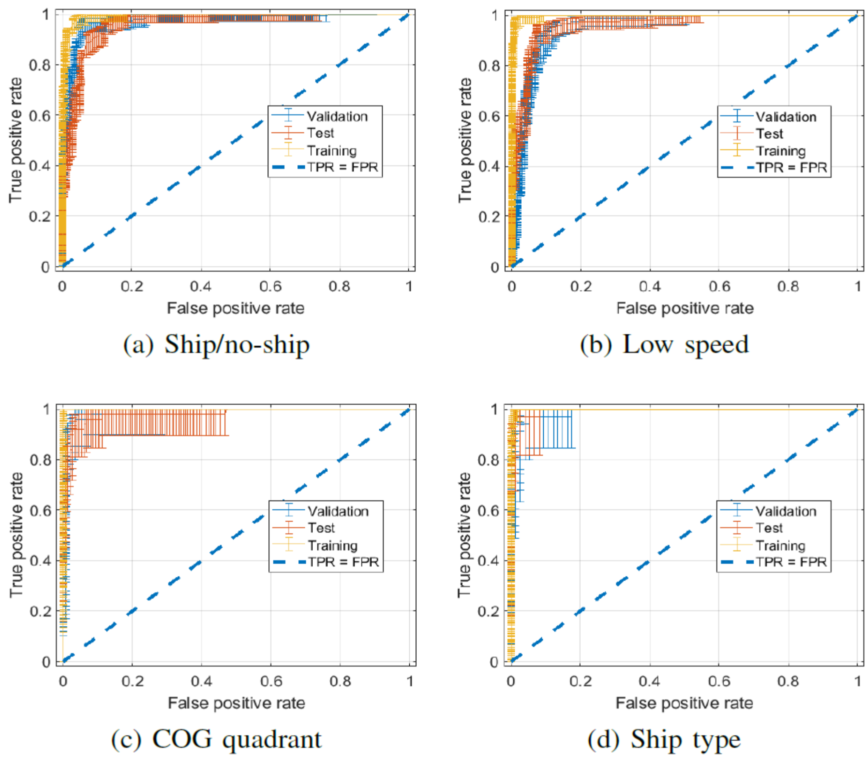

Figure 22: ROC curves of the four classifier considered in this work. The mean ROC curves and confidence intervals are estimated using a bootstrap procedure for the three data set training, validation and test.

4.3 Vessel detection in Sentinel-1 SAR imagery

Optical images (such as the Sentinel-2 images) often come with the issue of weather conditions affecting the quality of the information displayed in them (e.g., clouds covering vessels). The Sentinel-1 pair of satellites, on the other hand, are equipped with a C-Band synthetic aperture radar (SAR) imaging, enabling them to acquire imagery regardless of the weather. In this section, we present the approach to target detection and classification from SAR data.

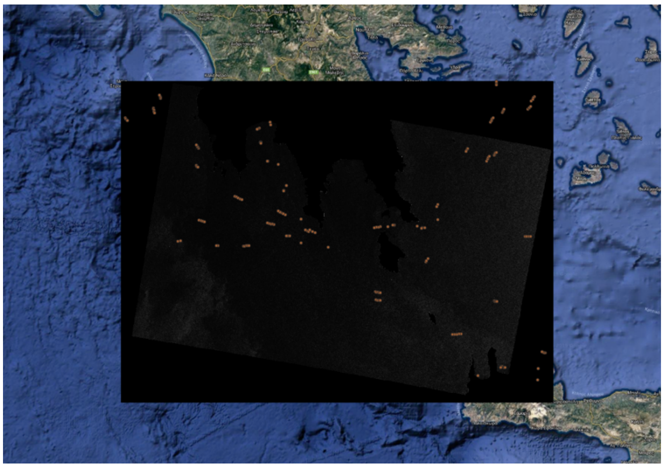

Figure 23: Example of Sentinel-1 image overlayed by AIS data (in orange colour)

4.3.1 Approach

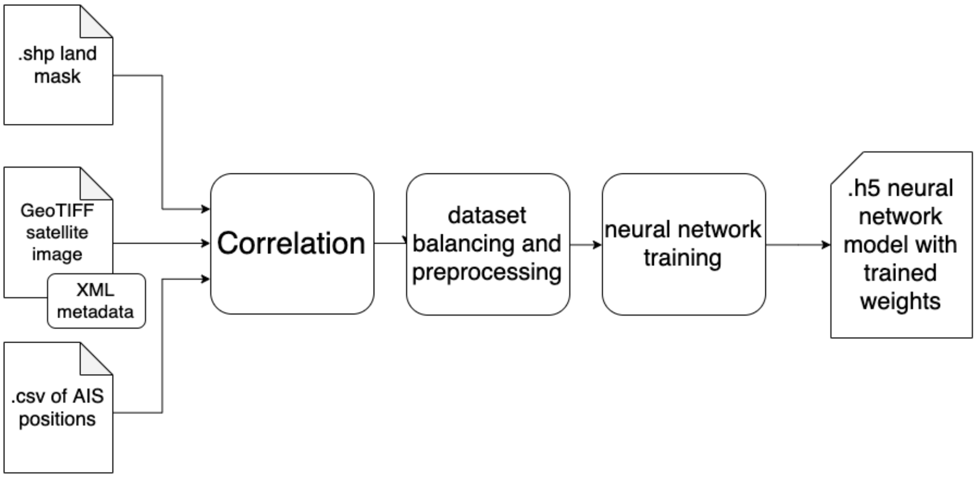

Figure 24: High level workflow

Figure 24 describes our workflow, that consists of several processing steps. These steps can be categorized as follows: (i) data correlation, (ii) processing and balancing, and (iii) training.

We used the Python package Sentinelsat to directly download the Sentinel-1 SAR satellite images from the Copernicus database. For the data processing tasks that are described below, we used the Geospatial Data Abstraction Layer (GDAL) python library, which is commonly used for geospatial operations. The process begins with re-projecting the satellite image to a standard projection (EPSG:4326). Afterwards, the land masking of the satellite image is performed in order to remove the land areas depicted in the image, which are out of interest and might affect the accuracy of our framework. As an input to the process, a polygonal shapefile that includes the area of the satellite image is required so as to mask out the land. This shapefile should include a polygonal area which represents all of the land of the area involved. Then, the shapefile is projected to the same projection system as the satellite image, clipped to the corresponding area, and then used to mask the land.

The AIS positions are then processed via linear spatiotemporal interpolation, so that the ships are in the approximate positions they were when the satellite image was taken, and subsequently are transformed into geometries. We use the AIS data to automatically annotate the images with respect to the presence or absence of a ship in a fragment of the image (a tile). We thereby show how a carefully designed data fusion process can be used resolve the problem of data labeling - oftentimes the bottleneck in many Machine Learning applications.

The next step is the correlation task, which is performed by splitting the satellite image into tiles. Each tile retains metadata about its corner coordinates, and thus after the tile generation, the tile's area is transformed into a geometry, and the intersection of the resulting geometry is calculated for each AIS position. That is to say, each AIS point geometry (which can optionally have a larger radius than the point itself, to account for irregularities and azimuthal ambiguities), is checked against the geometry that represents the area of each tile, so as to check whether the ship -- according to AIS -- is contained within the tile. The tiles are then marked accordingly for consumption by the neural network. In this way, AIS is considered the ground truth for the training of the neural network. This action is performed with every resulting tile. One of the parameters as input are the dimensions of the resulting tiles, which can be variable. Positions that are outside the bounds of the image post-reprojection and post-interpolation are discarded, and a distinction is made between "truly-empty tiles" (which have an average brightness of 0) and tiles that simply do not contain vessels (but contain background noise, waves, etc.). The former type of tile exists as due to the re-projection sections of the resulting image are "blank". Tiles of the former type are discarded.

Ultimately the task is modeled as a classic binary classification problem on satellite images (we use Sentinel 1 SAR images in this paper). The image classification task itself is handled by the CNN algorithm The result of this process is a set of ready-marked tiles for consumption by the convolutional neural network. In essence, the goal is for the neural network to be able to recognize the presence of a ship within a certain section of the satellite image. Specifically, it is a binary classification task of "ship(s) present/ship(s) not present". A convolutional neural network is used, instead of any other type, due to its inherent feature learning ability, i.e. its ability to capture relevant features from an image on different levels, similar to the human brain.

4.3.2 CNN

In the context of this work, as explained earlier, we used a convolutional neural network built using Keras. It is composed of 3 convolutional layers and 2 fully-connected layers, as shown in the figure below. Implicitly between each layer of the figure exists a ReLU activation layer. As an optimizer, Nadam was used (Adam optimizer with enhanced Nesterov momentum--one of the baked-in optimizers Keras offers), with a standard learning rate and other parameters. Dropout layers were used as well. This structure was experimentally found to bring the best results. As supervisory metrics, accuracy, binary cross-entropy loss, precision, recall, and F1 score were used. Early stopping was utilized to optimize the network's accuracy.

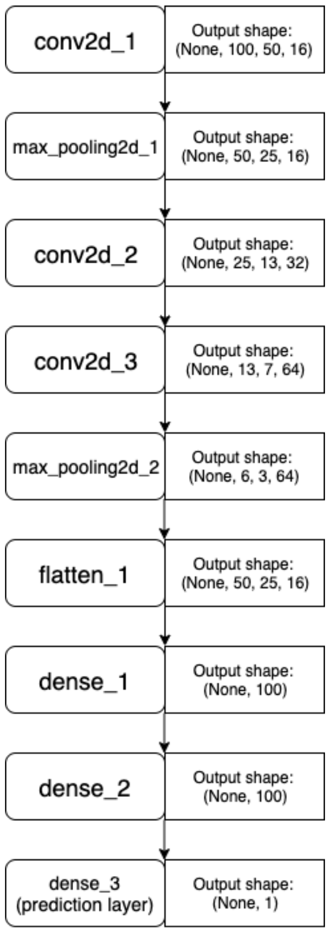

Figure 25: CNN architecture

4.3.3 Experimental evaluation

In this section we describe the preliminary experimental evaluation of our approach. Sentinel 1 is equipped with a SAR sensor, so the output images have the advantage of being unaffected by weather conditions due to the radar nature of the sensor. The images were taken primarily from two areas, south of the Iberian peninsula and the Aegean, due to both the fact that it has excellent terrestrial AIS coverage (to ensure that no ships are missing from the AIS data) and to the large amount of ship traffic that passes through both these areas, ensuring that the ships-per-image ratio was fairly high so as to extract as much value training-wise from each image as possible. The AIS data for each area was sourced from MarineTraffic.

The testing of the neural network was done on an image hand-correlated via QGIS taken from the Aegean sea, and as such it is certain that the labelling was done without any correlation errors. To perform this correlation by hand, the image was loaded into the QGIS software, and the AIS positions were overlaid on top of the image. The image was then split into tiles, and each tile that corresponded to an AIS position was marked at first as a ship tile. At this point, the process is the same as that which is done automatically through the methodology. However, the correlation by hand involved the further step of correcting the automatic process when the AIS positions did not correspond, due to azimuthal ambiguities or imprecise spatiotemporal interpolation, to the underlying position of the ship in the image, ensuring 100% accuracy in the correlation, something the automatic process does not guarantee.

The results are fairly promising, as shown in the table of Table 5. Compared to the model loss graph shown in Figure 26 and the model accuracy graph in Figure 28 the actual loss and accuracy are much higher. This is due to the fact that these graphs were generated based on the automatically correlated data, while the testing was done on the manually-correlated image which has a 100% guarantee of correct correlation. The threshold value, as shown in the table above, is the value above which the prediction of the neural network is considered to belong to the predicted class. For example, if the neural network gave an output value of 0.7, if the threshold were 0.5 it would be considered a positive result, but if the threshold were 0.8 it would not. In this way, by tuning the threshold value, it is possible to adjust whether higher recall or higher precision is given more weight, which is generally selected based on the nature of the problem at hand.

When tuning the neural network threshold in this case, higher recall (i.e. lower threshold) was preferred to higher precision. This is because in a real-world scenario, it would be more damaging to miss a ship (i.e., identify that no ship is in a region where one is, potentially allowing illegal activity to go unnoticed) than to classify as a ship something that is not (i.e., identify that a ship is in a region where there is nothing there). This also explains the discrepancy that seems to exist between the Area under ROC score and the accuracy. A higher accuracy could be achieved, as well as a higher (near perfect or perfect) precision, if a sacrifice was made with regards to the recall.

This led to the result of higher testing accuracy vs. the training and validation datasets, as the faults in the automatic correlation leads to noise in these datasets. This constitutes the primary challenge for this problem, as both the azimuthal ambiguities inherent in the SAR sensor and the occasional incorrect spatiotemporal interpolation lead to occasional incorrect correlations between AIS positions and the underlying image. The spatiotemporal interpolation is linear, and as such if the ship greatly changed heading or position this could affect whether the correlation is correct or not. It should be noted that the approach and methodology is fully generalizable to other types of satellite data, e.g. non-radar based/optical types, in which case this noise would not be present and the accuracy would likely be higher. More details about the work described above can be found in [46]

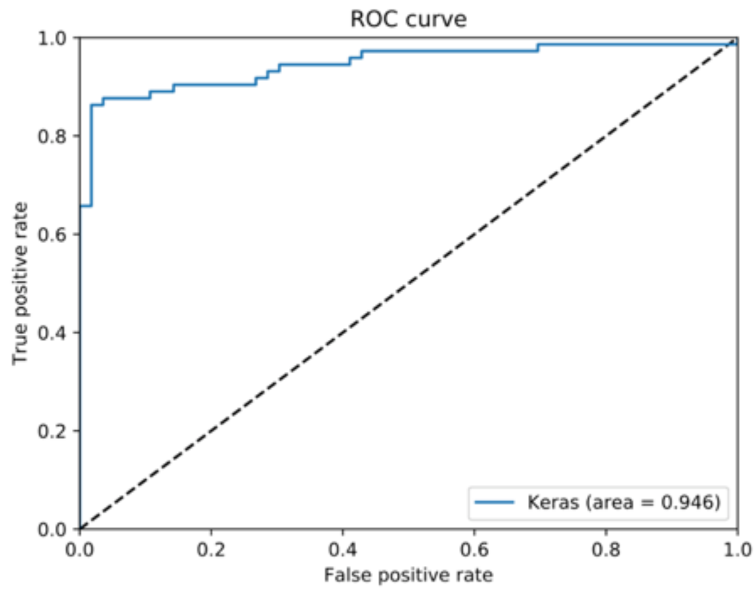

Figure 26: Model ROC curve

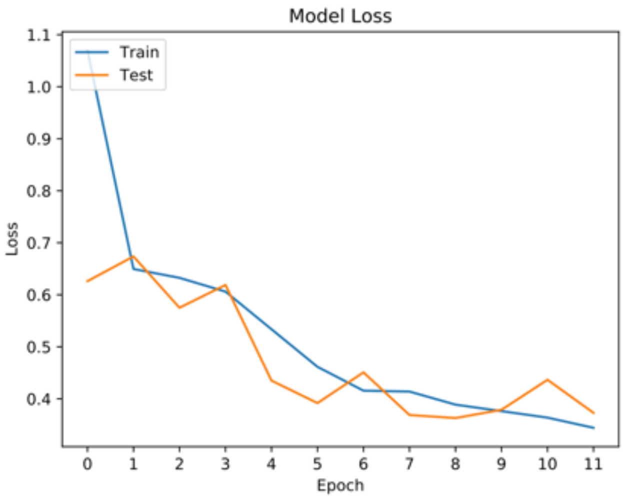

Figure 27: Graph of the model loss function vs epoch

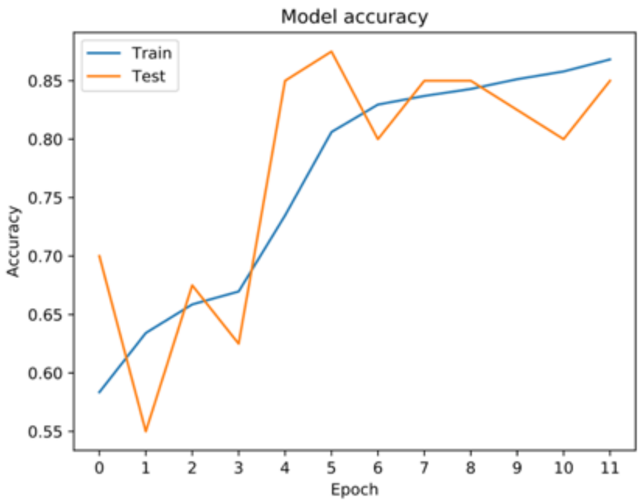

Figure 28: Graph of the model accuracy vs epoch

Table 5: Results from the best model

Threshold	0.30
Area under ROC score	0.946
Accuracy (%)	0.884
Accuracy (number of correct identifications from test set)	114/129
Precision	0.892
Recall	0.904
F1 Score	0.898

5 Local/global view integration platform

The data streams from the local and global view sensors are integrated into the maritime situational awareness platform described in the following subsections. The interface between the single sensor component and the situation awareness platform is implemented by means of target contact messages in XML or JSON format that contains information about the location and identity of the contact detected by a sensor plus other information that is relative to the sensor platform from each the message is originated. An example of such a message is provided in Appendix II and it is relative to the interface between the CMRE adaptive robotic sensor network described in section 3.1 and the situational awareness platform system (see Figure 29 for an example of system configuration).

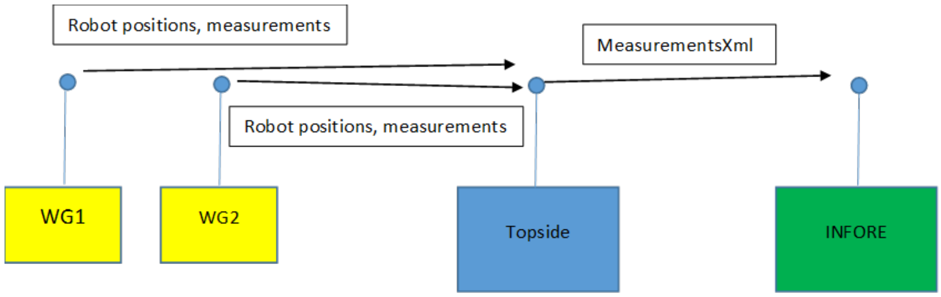

Figure 29: Message exchange between the adaptive autonomous CMRE sensor network and the INFORE situation awareness system. Here the Topside is a command and control centre that integrates the measurements form the robots in the field and transmit the contact measurement file to the INFORE platform for situation awareness.

5.1 INFORE Maritime Situational Awareness Sensor Network Ontology

The INFORE Maritime Situational Awareness Sensor Network Ontology is designed to annotate and semantically enrich the data generated by the heterogeneous sensor network in support of the INFORE maritime use case. It can be extended to other Maritime Situational Awareness scenarios not currently considered in this use case, and the design patterns applied in its design are potentially applicable to situational awareness in general.

In particular, the ontology models sensors, observations, data streams, observations values, and any information that can be extracted from them as a result of analysis for supporting decisions.

As presented in sections 3 and 4, INFORE maritime sensors include AIS, remote sensing, acoustic sensors, thermal camera, and radar. Following an established pattern in sensor modelling [19], in the ontology the concept of sensor is extended beyond physical sensors to include virtual sensors like software and human sensors (e.g., maritime operators). Similarly, other sensors can be included (e.g., news, social media, reports)

As described in sections 3, 4 and 5.2, information resulting from the analysis of sensor data includes analytics results like target detection and classifications, maritime events, anomalies and maritime activities detected from data. All these concepts are represented in the ontology. As a consequence of the proposed extension of the concept of sensor, the second order information produced by data analytics is modelled as a particular type of observation. This design choice, which models seamlessly sensor data and analytic results, allows recursivity and enables a straightforward representation of data processing workflows. Data provenance is modelled as well. At any instant in time, the underlying knowledge graph is a comprehensive representation of the maritime situation as for the underlying sensor network, and awareness can be updated accordingly.

An important aspect of the proposed ontology is the modelling support for information quality. Uncertainty on sensor observations and analytics result is modelled explicitly as a particular type of observation, which is linked to the originating data and the originating sensor. Since in situational awareness the concept of quality applies also to sensors, and quality assessment may be accomplished by a different sensor than the one generating the data, both observations and sensors are modelled as observable features of interest. The proposed model of sensors, observations and their quality enables a complete and effective representation of all the pieces of information contributing to situational awareness.

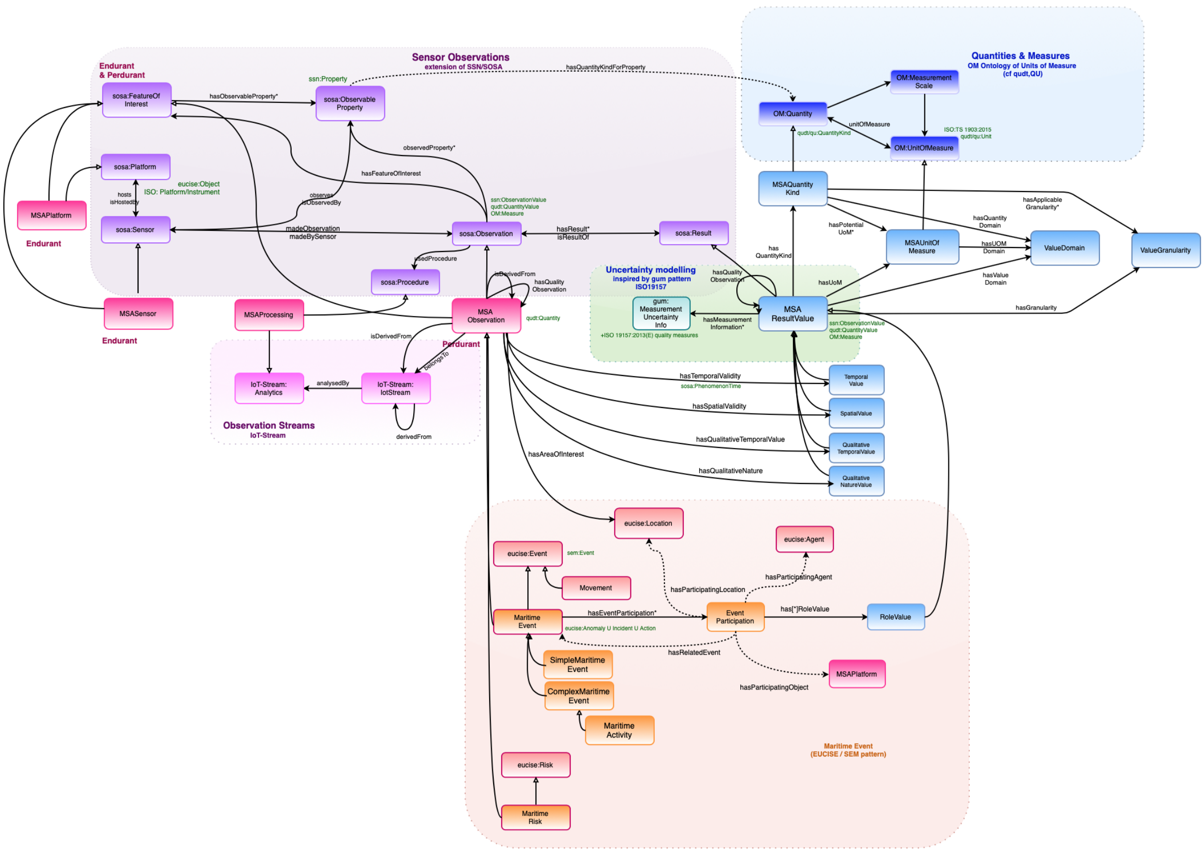

Figure 30: Excerpt of the INFORE Maritime Situational Awareness Sensor Network Ontology, describing the top-level concepts for sensors and observations, data streams, values, and processed data. The INFORE ontology aligns with references ontologies and data models in the respective areas, as highlighted with colored background: SSN/SOSA [19] and IoT-Stream [20] for sensors, observations and observation streams; OM [21] for measures, units, EUCISE [25] and SEM [26] for maritime events and data modelling.

Figure 30 shows an excerpt of the top-level concepts of the ontology, and highlights the alignment with reference ontologies and data models for sensors and observations, data streams, values, and maritime events, as described in the following section.

5.1.1 Background

The ontology extends existing ontologies defined for sensor networks and maritime data exchange. The modelling of the data acquisition from the heterogeneous sensor networks relies and adapts the formalisation proposed in SSN/SOSA for sensors, sensor observation and processing [19]. The modelling of observation stream and stream analytics is mutated from IoT-Stream [20].

The ontology aligns and extends the Ontology of Units of Measure and Related Concepts (OM) [21] to represent sensor values, quantity kinds and units. Analogies with other ontologies for quantities and units of measures like the QUDT CATALOG of Quantities, Units, Dimensions and Data Types Ontologies[6] may be also highlighted.

The OM's pattern for quantities and measures has been extended to model sensor and processing result values of any kind, including quantitative, descriptive, quality assessment, spatial and temporal elements [22]. The annotation of values with quality information corresponds to the one defined in [23], and can be extended to include also other types of quality measures (e.g., the quality measures defined in ISO 19157:2013(E)).

[6] http://www.qudt.org/2.1/catalog/qudt-catalog.html

The ontology leverages the specification of maritime events of the Common Information Sharing Environment (CISE), as formalised in the EUCISE-OWL ontology [24] to implement the official EUCISE data exchange model[7]. This event model relies on the Simple Event Model Ontology[8] [25], which is widely adopted in the literature also for the representation of marine data collection and events (see the GeoLink Modular Oceanography Ontology - GMO) [26].

5.1.2 Ontology Design

Sensor and sensor observations. As illustrated in the top-left of Figure 30, in the ontology, the concepts infore:MSASensor and infore:MSAObservation and the related entities extend the pattern defined in SSN/SOSA for sensors and observations. As such, sensors observe properties (sosa:ObservableProperty) of entities (sosa:FeatureOfInterest). As for SSN/SOSA, any infore:MSAObservation results from the execution of a sosa:Procedure, i.e., a physical sensor plan or algorithm. MSA analytics include in-situ, ex-situ and remote sensing processing.

Any infore:MSAObservation is a structured and annotated representation of an infore:MSAResultValue, defined as extension of sosa:Result, representing a measure or an estimate of some entity property. Differently from SSN/SOSA, in the ontology qualitative measures are supported as well.

Any infore:MSAObservation is associated to an area of interest, modelled as eucise:Location, and its evaluation is bounded in space and time (as infore:SpatialValue and infore:TemporalValue, representing sets of spatial values of the same type and set of non-contiguous time intervals expressed at the same granularity). Other temporal annotations include the execution/observation timestamp (sosa:ResultTime) and its qualitative temporal validity (i.e., whether the observation is a nowcast, a forecast, or a re-analysis). Some qualitative information on the nature of the observation (e.g., observed, estimated, simulated) may also be represented.

The concept infore:QualityObservation represents quality information like uncertainty on observations and sensors (e.g., credibility, reliability), to include quality evaluation on observations, sensors, analytics or processing. Imprecisions and resolution may also be represented. Any MSA observation may be directly associated with all its quality evaluations, and the generating sensors and the associated quality evaluations may be retrieved as well, for a comprehensive evaluation in the fusion system.

The support for provenance includes the annotation of observations with the generating sensor and with the originating observation, whenever the observation is the result of a workflow execution (i.e., analytics results may be associated with raw data from physical sensors, or other pre-processed data).

Observations may be gathered in a IoTStream:Stream, following the IOT-Stream pattern, which can be further analysed. Stream analytics and procedures are extended by the concept infore:MSAProcessing for the use of the INFORE use case.

Quantities and Measures. Each infore:MSAObservationValue is characterised according to its class which gives the value representation, but is also annotated according to an infore:MSAQuantityKind, which defines the dimension the value measures, associated to a infore:MSAUnitOfMeasure. Both concepts extend the corresponding concepts in OM, i.e., om:QuantityKind and om:UnitOfMeasure. These are extended with additional relationships with infore**:**ValueDomain and infore:Granularity. gum:

gum:MeasurementUncertaintyInfo can be associated to a value to represent quality annotation (e.g., the type of evaluation applied to assess the confidence on the value; the uncertainty function applied).

Maritime Events. Detected, estimated or forecasted maritime events are modelled in extending and aligning with the CISE/EUCISE model and the corresponding ontology. The concept infore:MaritimeEvent extends eucise:Event and groups different types of events, from simple events to complex events and maritime activities. Events defined in EUCISE like anomalies, incidents, actions may be represented as specific complex events. Each infore:MaritimeEvent links to associated instances of eucise:Location, representing the area of interest of the event (e.g., a port), the platform of interest (e.g., a vessel), the agent and the associated events. These relationships are expressed according to roles as for the EUCISE specification. The roles are formalised as descriptive values (infore:RoleValue). Each infore:MaritimeEvent is an infore:MSAObservation. As such, each event is valid in a specific time and space.

[7] http://www.eucise2020.eu/media/1131/d4_3-Appendixb.pdf
[8] https://semanticweb.cs.vu.nl/2009/11/sem/

The maritime events of interest for INFORE include simple and complex events as described in section 5. Simple events correspond to maritime situational facts as defined in [27] and simple maritime situational indicators as defined in [28]. Complex events represent maritime activities, anomalies and complex situational indicators, according to [27][28][29][30].

5.2 System for situation awareness and event prediction

In this section we describe the MSA workflows that are being implemented in INFORE. Figure 31 shows the INFORE workflow of the MSA use case. The components that take part in the workflow are the described below.

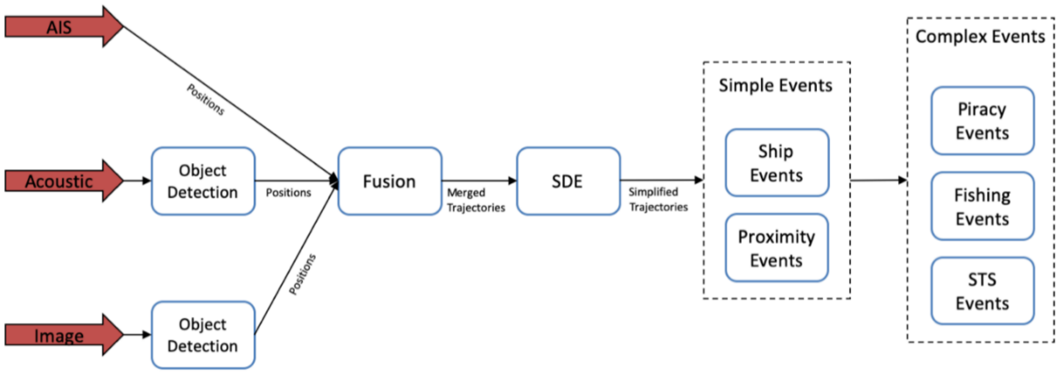

Figure 31: Workflow for the MSA use case of INFORE.

5.2.1 Fusion

Data fusion takes place so that the positions of vessels coming from heterogeneous sources are merged into trajectories. For example, positions of vessels that are not covered by AIS (e.g., because the vessel may have its transponder switched off), are complemented by the positions of the same vessels identified in acoustic/imagery/radar data. The output of the fusion operator will be the merge trajectories for each vessel, containing positions from different sources of data.

5.2.2 The Synopsis Data Engine (SDE)

The merged trajectories of the previous step are then forwarded to the SDE component. This component is responsible for constructing synopses of the data in order to reduce their volume and decrease the execution time of computations. In this case, the positions contained in each merged trajectory are downsampled, creating a synopsis that keeps the "highlights", i.e., the critical points of each trajectory, skipping positions that are spatiotemporally similar to other positions of the vessel and/or have the same navigational status (i.e., there are no turns in between), so that there are no significant changes in the pattern of the vessel behaviour that is computed from the synopsis compared to the one computed from the original data. Thus, the output of this operation is a set of simplified trajectories.

5.2.3 Simple event detection.

This component detects maritime events that are simple in the sense that they are not composed of other events and it is implemented as a distributed system that is currently deployed in the MarineTraffic Akka cluster. The architecture of the system is shown in Figure 32. It follows a version of the Lambda architecture that consists of a batch layer and a real-time layer. The batch layer takes as input massive historical AIS data for the global fleet in order to cluster all the positions of vessels that have navigated along port-to-port routes. In this way, for each, and given a pair of origin and destination ports, we know all the "common" routes that most vessel types follow. The real-time layer takes as input streams of real-time AIS data, i.e., the "current" positions of all vessels in the world and detects events that deviate from common behaviour in real-time. For example, if a vessel deviates from a common route followed from most of the other vessels of its type for the same pair of origin and destination ports, a route-deviation event occurs. To increase performance, the Actor model is used, implemented in Akka. Every vessel Actor is assigned to each vessel of the global fleet. Also, space partitioning is used using a grid, with each actor being assigned to each grid cell. In this way, each vessel belongs to a grid and there is an actor responsible for storing navigational information about the vessel and another actor is responsible for maintaining the most up-to-date state of the grid cell.

The simple maritime events that are currently supported are the following:

- *Drifting.* A vessel drifts when there is a difference between the course over ground (Cog), which is the direction of the path of the vessel, and the heading of the vessel (i.e., the direction of its bow). A vessel may drift due to weather and sea conditions (e.g., wind, tides, etc.) and/or due to its navigational status (e.g., anchored). As we describe in the next section, a drifting event is important to identify a fishing event.
- *AIS-off.* AIS-off is an event that occurs when a vessel suddenly stops transmitting signals for a period of time. This communication gap might occur due to (i) low coverage in the area, (ii) equipment (i.e., transponder) malfunctions, and (iii) intentional switch-off of the AIS transponder of the vessel by the crew so that the vessel cannot be tracked (e.g., engaging in illegal activities). For this reason, the AIS-off event can lead to the detection of more complex events.
- *Proximity.* This is an event that occurs when vessels are located in close distance to each other. This might happen due to an imminent collision or due to a narrow passage or due to the fact that the vessels are about to "collaborate" (e.g., tugging, piloting, ship-to-ship transfer of cargo, etc.). This is an important event that forms the basis of many complex events as we describe in the following section.
- *Route deviation.* The *route deviation* event occurs when a vessel spatiotemporally deviates from common routes that most vessels of its type follow for the same voyage (i.e., same pair of origin and destination ports). Apart from the spatiotemporal criteria used to determine whether there is a route deviation, other statistics are also used, which are related to the overall vessel behaviour. For example, a vessel might have significantly lower or higher speed compared to other vessels of its type during the same voyage in the same area (i.e., the same convex hull).

The simple events detector is integrated into the Anomaly Detection tool of MarineTraffic, that also includes a Web user interface. A snapshot of the interface is shown in Figure 33, showing simple maritime events occurring worldwide. The proximity events are shown in red colour, the AIS-off events are shown in blue colour, and the route deviation events are shown in light blue colour.

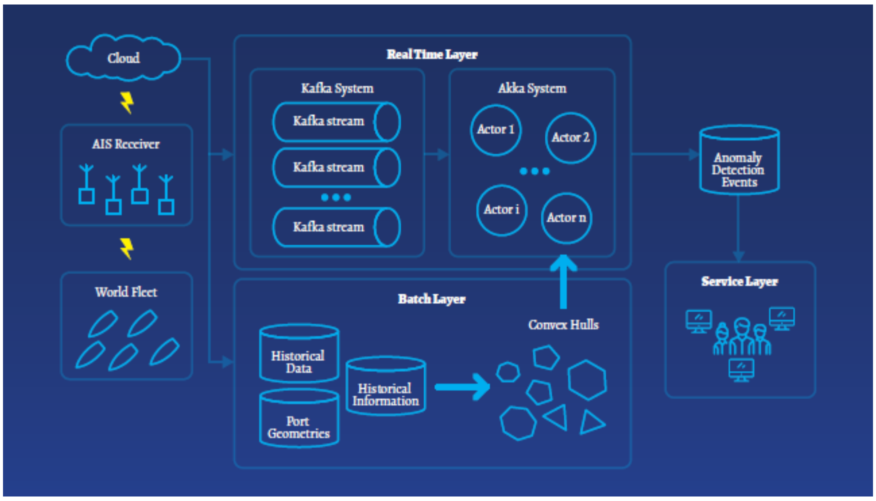

Figure 32: Distributed architecture for the detection of simple events.

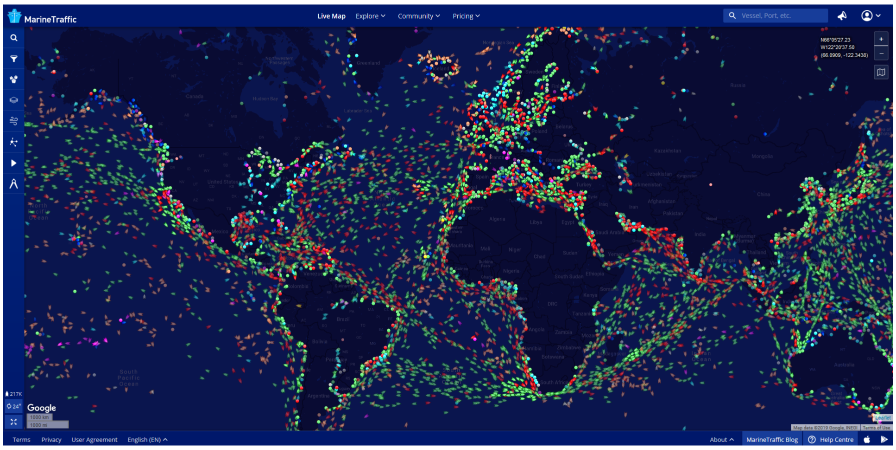

Figure 33:Anomaly Detection events at global scale.

5.2.4 Complex activity classification

Complex activities (or events) are activities/events composed of simpler ones. For example, a proximity event, i.e., an event that is triggered when two or more vessels are close to each other, might happen in a context of a more complex event that requires that vessels are close to each other, such as piloting, ship-to-ship transfer, etc. In the following, we provide definitions for some complex vessel activities (events) that involve some of the simple events described in the previous section.

- Tugging: Tugging is an event that occurs when a vessel tugs another vessel. In most cases, a small vessel tugs a large vessel (e.g., a tanker) in order to provide navigation assistance in narrow passages and ports with traffic where it is difficult/unsafe for large vessels to navigate.
- Piloting: Piloting is an activity that aims for providing assistance to large vessels in order to enter ports with safety by maritime professionals that are experts in navigation inside the specific port. In this case, the boat that carries the pilot leaves the port, stops next to the vessel, the pilot boards the vessel and guides the vessel to the port. Then, both the boat and the vessel enter the port
- Ship-to-Ship transfer: This is an event that describes the transhipment of cargo between two vessels. In most cases, cargo is transferred in shore-based terminals equipped with the corresponding facilities but loading/discharging can also take place between two (or more) vessels at sea.
- Fishing:. This event denotes that a vessel is engaged in fishing activities.

5.2.5 Classification of trajectory patterns

One of the most important vessel activities that we want to be able to detect and forecast, is fishing. In this way, we will be able to timely detect and forecast fishing activities in prohibited/protected areas where fishing is not allowed. Fishing can be considered as a complex maritime event in the sense that it is composed of a combination of other events as we describe in the following sections.

The first step is to distinguish the different fishing activities, as different fishing activities correspond to different trajectory patterns. We consider the following two fishing activities: Trawling and longlining. The differentiation between these two fishing activities (and the corresponding patterns) is described below.

Trawling. Fishing vessels engaged in trawling activity (see Figure 34) use a fishing net located in the stern of the boat, called trawl, which is dragged through the water. The net is typically pulled by one or more fishing vessels, either on the sea floor (i.e., bottom trawling) or mid-water (i.e., mid-water or pelagic trawling), although single-boat trawling is usually the case. In single-boat trawling the spread of the net depends on the trawl doors, also called ”otter boards" and act as wings. To keep the wings steady the vessel must be travelling at a constant speed and for that reason, during trawling, vessels usually sail with lower steady speeds.

Figure 34: Typical trawling pattern

Longlining. During this type of activity (see Figure 35) vessels set multiple fishing lines with baited hooks attached to them, called snoods. The length of the fishing lines can reach up to a kilometer, while the total length of all the fishing lines in the entire activity can reach up to several kilometers. The lines can be deployed either near the surface (i.e., pelagic longline) or along the sea floor (i.e., demersal longline). While setting the lines, vessels travel at their steaming speed or slightly less and they maintain a constant speed. When all lines are set, they are left in the water for several hours and the vessel drifts slowly with them. To retract the lines, vessels follow the same procedure as when setting the lines. The process of setting the lines, waiting and retracting the lines can be repeated several times before returning to a port.

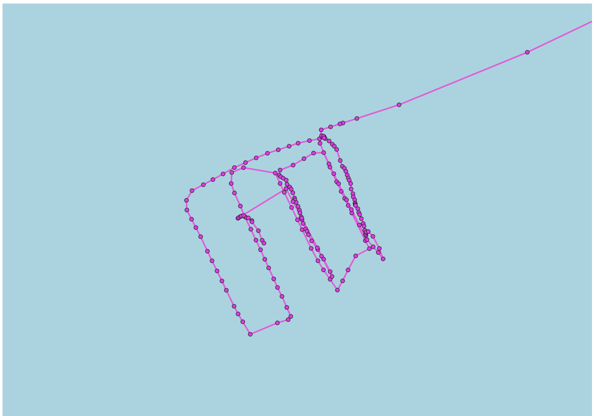

Figure 35:Fishing pattern that typically corresponds to longliners.

The patterns that correspond to both types of fishing activity, that are shown in Figure 34 and Figure 35, characterized by frequent manoeuvres and turns so that vessels stay close to the fishing area. The main difference of these two types of patterns is that trawling patterns consist of more manoeuvres than longlining patterns, which include parts of more straight lines followed by sudden turns. To be able to have a better understanding for the different patterns, we conducted a statistical analysis against an annotated AIS dataset that we used as ground truth and observed the speed and number of turns of vessels while engaged in fishing activities as compared to being underway (e.g., navigating into the sea towards a destination).

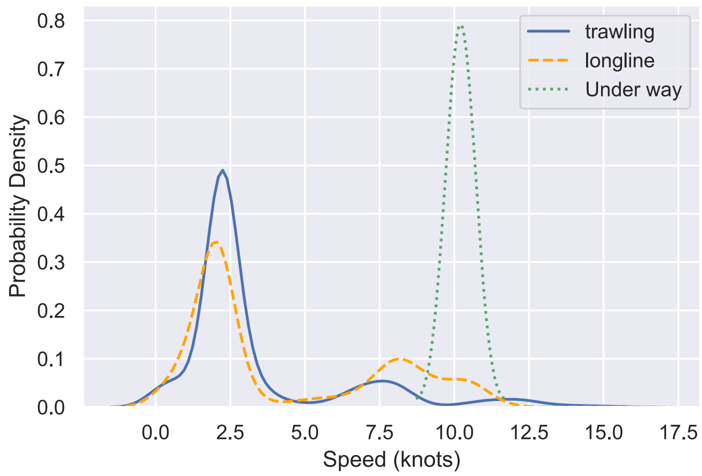

Figure 36: Speed distribution while in trawling, longlining, and underway vessels.

Figure 36 shows the speed kernel density distribution of vessels while trawling, longlining and navigating towards a destination (i.e., under way). Figure 37 shows the distribution of number of turns involved in the trajectories of vessels engaged in the aforementioned activities. In both figures, the distributions of trawling vessels appear in blue colour, the distributions of longliners are marked in orange colour, and last, the distributions of under way vessels are marked in green colour. Reasonably, the speed of vessels that are under way to a destination is higher than in the cases when the vessels are engaged in fishing. On the other hand, both trawlers and longliners follow similar speed patterns. Both types of fishing activity have two peaks in their speed distribution, the first one being in the range of 1-3 knots and the second one being in the range of 7-10 knots. More specifically, it can be observed that the speed of trawlers is more likely to fall into the first peak than the speed of longliners. A similar pattern can be observed for the second peak as well but with the longliners' speed now having higher probability density. Furthermore, in longlining activity, the first peak is slightly shifted to the left and the second peak to the right compared to the trawling activity. This can be explained because longliners have higher speeds when setting the lines and the duration of the process takes up a large part of the longlining activity. Moreover, they have lower speeds (i.e., 1-3 knots), compared to the trawlers, after setting the lines and before retracting them, which indicates that they remain stationary drifting along with the lines.

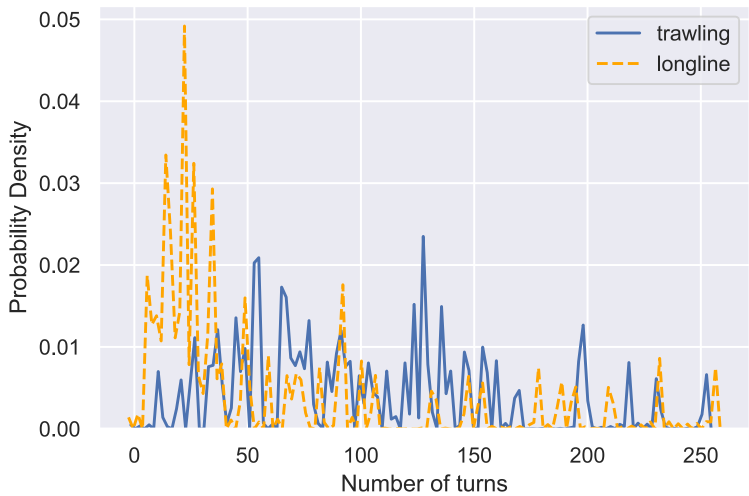

Figure 37: Number of turns while in trawling, longlining, and underway vessels.

5.2.6 Feature engineering

- To build our Machine Learning model, we consider the following features:

- *Average speed*: The average speed during a vessel's trajectory.
- *Standard deviation of speed*: This feature measures the "steadiness" of the speed along the trajectory of the vessel.
- *Average drifting*: Drifting is a **simple event** that can be detected when there is a difference between the course over ground (Cog), which is the direction of the path of the vessel, and the heading of the vessel (i.e., the direction of its bow). A vessel may drift due to weather and sea conditions (e.g., wind, tides, etc.) and/or due to its navigational status (e.g., anchored).
- *Standard deviation of drifting*: This indicator shows changes in the drifting status of a vessel.
- *Standard deviation of Course over Ground*: This is an indicator that shows to which extent the trajectory of a vessel maintains a steady course (i.e., it moves on a straight line).
- *Number of turns*: The number of turns of a vessel during a trajectory.
- *Accumulated angle*: The sum of degrees of the angles that a vessel turns by the time it starts to the time it stops turning during a trajectory.

5.2.7 Classification model

The algorithm that we chose in order to train our model using the features described in the previous section to this end is the Random Forest (RF) classification algorithm due to its high performance results in the maritime domain [37][38] and because RFs combine the predictions of many Decision Trees into one model, thus they are less prone to overfitting [48]. Furthermore, a Random Forest classifier is less computationally expensive than Decision Trees, creating a good basis for online predictions or online re-training. Finally, Random Forests require far less data than other state of the art algorithms such as Neural Networks and it is easier to interpret their predictions based on the features [39] which in an industry setting, such an interpretation gives meaning to interested stakeholders.

5.2.8 Classification of vessel events against real-time streams of maritime data

Figure 38 illustrates a high-level overview of the system architecture that performs real-time vessel activity classification against streams of AIS data from MarineTraffic.

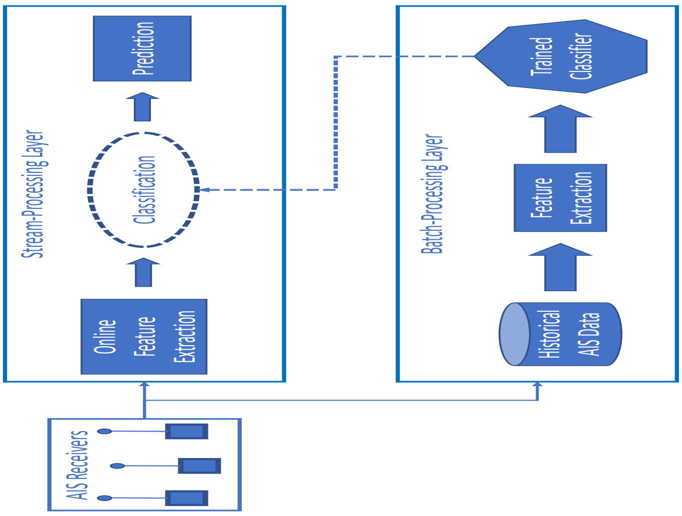

Figure 38: High level overview of vessel activity classification.

The system architecture illustrated above consists of the following layers: the batch-processing layer and the stream-processing layer.

The batch-processing layer extracts features from the historical AIS data and trains a classifier. The stream-processing layer consumes AIS messages from the receivers and makes a prediction by using the pre-trained classifier generated from the batch-processing layer. The workflows performed in each layer are described below.

Batch-processing layer.

In the batch-processing layer, the model is trained using the Random Forest algorithm as described above. To achieve this, we used an AIS annotated dataset provided by MarineTraffic. This dataset contains trajectories of vessels that are either engaged in a fishing activity (i.e., trawling or longlining) or they are under way to a destination.

This layer is responsible for the construction of the Random Forest classification model. For the training of the model, ground truth trajectories are required. The features described in the previous section are extracted, and the output is used to train the RF classifier. The implementation is written in Scala and it is based on the Statistical Machine Intelligence and Learning Engine (SMILE) library[9], which is known for its performance and optimized utilization of resources (e.g., memory consumption), as well as its compatibility with our existing architecture which is implemented in Scala. According to a third-party benchmark[10], SMILE outperforms R, Python, Spark, H2O and xgboost significantly.

Stream-processing layer. In order to achieve high-throughput, low-latency performance, the stream-processing layer is implemented in the Akka[11] framework which takes advantage of the Actor model [40]. Actors in the Akka framework exploit the concurrency capabilities of threads, they are lightweight, and millions of actor instances can be deployed in a single machine since they have a small memory footprint (i.e., 2.5 million actors per GB of heap). To assist the implementation of the classification of fishing activity, one type of actor from the architecture is used, namely the Vessel Actor.

The Vessel Actor is responsible for consuming AIS messages originating from a single vessel and classifying parts of its trajectory based on the model created from the batch-processing layer. Thus, each vessel has a dedicated actor which is created after the first AIS message has been received. The actor remains idle and acts only when a new message is received. To classify parts of a trajectory of a vessel, each actor takes into account features extracted from an event-based window of user-defined length. To reduce memory consumption, features are extracted online, thus the need of storing a batch of AIS messages is eliminated.

When a window is complete, all indicators have to be computed again for the next window. After all features have been extracted, they are fed to the RF model which outputs a decision along with its probability, indicating the activity the vessel performs at the current window. Figure 39 illustrates the online calculation of the average speed. At each incoming AIS message a new average is calculated. The new average speed calculated based on the last AIS message, represents the average speed of the entire window. When the last AIS message of the window is received, the classification is triggered.

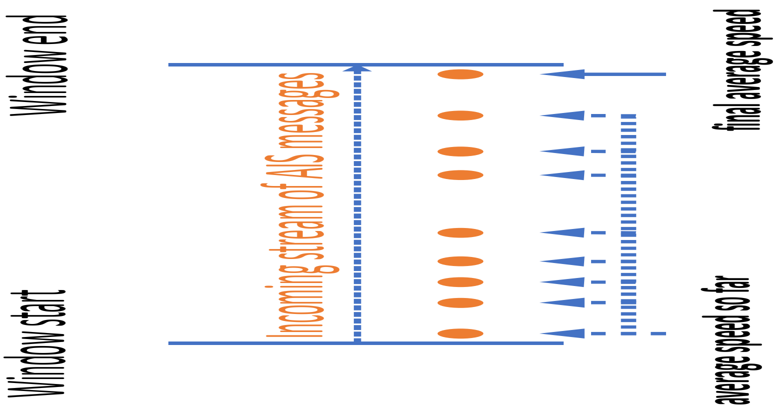

Figure 39: Online calculation of average speed.

5.2.9 Experimental evaluation

In this section we present the set up and the results of our experimental evaluation.

Workload

[9] https://haifengl.github.io/
[10] https://github.com/szilard/benchm-ml
[11] https://akka.io/}

For the experiments we used a MarineTraffic dataset that contains AIS messages during a two-month period (1/1/18-28/02/18) that covers the seas of Northern Europe. The AIS messages used for our ground truth dataset contain fishing activities that have been extracted from vessels which have set their navigational status to 7, which indicates ``fishing activity'', and by vessels which have set their destination to Trawling or Longlining for the corresponding activity. These fishing trajectories are then segmented to fishing or non-fishing segments. The total number of AIS messages sums up to 61,050, 16,110 of which related to vessels engaged in trawling activities, 8,484 related to longlining activities, and 36,45 messages of vessels that were under way. Although, the number of messages per activity varies, the number of events per activity remains the same. This is due to the transmission rate of the AIS protocol. When vessels travel at high speeds, the frequency can get as high as one message every two seconds, while the lowest frequency can get as low as one message every 3 minutes when the vessels are not moving. Since the underway vessels travel at much higher speeds, the number of AIS messages is also increased. Another factor affecting the AIS transmission rate is the vessel's turn frequency. Since trawling activity is characterised by frequent turns, the number of AIS messages will be higher compared to the longlining activity but not higher than the messages of the underway activity since the speed during trawling is much lower.

Experimental set up and results

We evaluated our implementation using three different experimental set-ups:

1. **RF parametrization**. We conducted experiments using with different configurations of the RF algorithm and evaluated its performance and accuracy with respect to well-known metrics (e.g., f1-score, accuracy etc.) in order to assess the influence of the performance of the model using different combinations of hyperparameters. More specifically, the first hyperparameter selected is the number of trees of the forest. We used three distinct configurations for the number of trees (10,50,100} and run 5-fold cross validation per setting. The idea behind the Random Forest algorithm is to optimise the prediction of an instance by averaging the predictions of multiple decision trees. Moreover, for each configuration, we tested three distinct configurations of another hyperparameter of Random Forest, the maximum depth, setting its value to 2, 5 and 10 respectively. This parameter controls the size of the trees, specifically defining the maximum number of levels each tree in the forest can have. Figure 40 shows the results of each experimental setting. From the results, we observe that the configuration with the highest classification performance is 100 number of trees and 10 as maximum depth that achieves f1-score of 93.52 and accuracy of 95.33. Therefore, for the rest of the experiments we use this configuration of RF parameters.

number of trees	maximum depth	Accuracy	Precision	Recall	F1-score
10	2	72 %	64.02 %	68.05 %	65.97 %
50	2	74.66 %	62.07 %	65.01 %	63.5 %
100	2	77 %	64.5 %	66.22 %	65.34 %
10	5	89.66 %	84.76 %	88.24 %	86.47 %
50	5	90.66 %	88.13 %	89.81 %	88.96 %
100	5	91.33 %	85.64 %	88.22 %	86.91 %
10	10	92.66 %	89.02 %	88.75 %	88.88 %
50	10	93.33 %	87.71 %	91.91 %	89.76 %
100	10	95.33 %	93.91 %	93.15 %	93.52 %

Figure 40: Results of the first round of experiments.

2. **Varying temporal windows**. We evaluated the robustness of the classifier when we change the length of the temporal windows. More specifically, we segmented each trajectory into temporal segments of 1, 2, 4, 8, 12 and 24 hours. This means that a fishing activity, e.g. trawling is now segmented into more parts, according to the temporal size. For each temporal size we performed 5-fold cross validation, keeping 80% of the trajectories as a training set and the rest 20% as a test set. The results of this round of experiments are shown in Figure 41. We can observe that the accuracy is increased as the time window length is increased. Furthermore, it can be seen that from the one-hour window length to the four-hour, the accuracy does not show any significant change, while from the four-hour window length to the twenty-four-hour, the accuracy increases abruptly, from 82.53% to 89.54%. This can be explained due to the fact that a fishing pattern may take hours to form. The features of each trajectory start to become distinguishable from one another after several hours have passed. Our findings show that that the time threshold with which a pattern in the fishing trajectory is formed needs to be at least four hours which explains the increase in the accuracy.

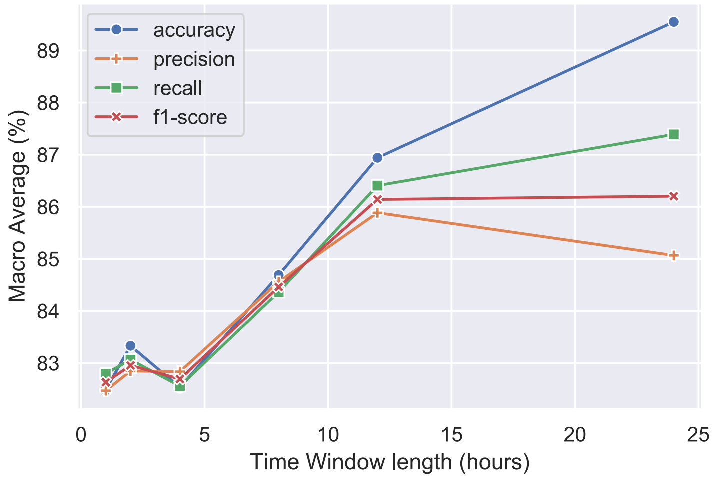

Figure 41: Experiment results for the second round of experiments.

3. **Comparison with related approaches**. Finally, we compare the classification performance of Random Forests against other well-known classifiers, such as the Gradient Boosted Trees (GBT), the Linear Discriminant Analysis (LDA), and Logistic Regression, using the same set of features. For the Gradient Boosted Trees we used the same hyperparameters to the Random Forests, since both of these classifiers use multiple decision trees to make a prediction, thus making a more fair comparison between the two. For the rest of the classifiers, we used the default hyperparameters that are provided by the SMILE library. The results of this round of experiments are shown in Table 6. We can observe that Gradient Boosted Trees slightly outperform the Random Forests, yielding the best classification performance (a F1-score of 87.29%), while both the LDA and the Logistic Regression perform weakly. A more in-depth comparison between the classifiers by fine-tuning the classifiers' hyperparameters will be conducted in the future for a more thorough evaluation. More details about this work can be found in

Table 6: Average results per classifier.

Classifier	Accuracy (%)	Precision (%)	Recall (%)	F1-score (%)
Random Forests	89.54	85.06	87.38	86.2
Gradient Boosted Trees	90.98	86.77	87.83	87.29
Linear Discriminant Analysis	81.4	69.13	77.71	73.17
Logistic Regression	79.71	76.19	75.59	75.89

5.3 Designing workflows for maritime data processing using RapidMiner

One of the objectives of this use case is to enable the integration of the components described above into workflows using a user-friendly and interactive graphical interface, such as the RapidMiner environment. Below we provide screenshots of two example workflows.

Workflow 1, shown in Figure 42, retrieves streams of maritime data via the local Kafka sub-cluster of MarineTraffic. Then, the Maritime Event Detection component identifies events on these streams, and then filters are used in order to keep only the events of interest (as for example the events "proximity_start" and "proximity_end"). Last, the Sink operator is used to write the corresponding types of events into the respective output Kafka topics. Workflow 2, which is shown in Figure 43, differs from Workflow 1 in that it includes also the Synopsis Data Engine operator, which takes the input AIS streams of data as input and outputs data synopses that are fed to the Maritime Event Detection operator. The SDE, as we explained earlier, is very useful in order to downsize the input streams of data and keep the important information which is forwarded to the next step, improving performance. It is noted that in the time of writing this document, Workflow 2 is not fully functional with respect to the UI, but the technical issues have occurred are expected to be resolved in the following weeks, however it works in the back-end level (i.e., the components are integrated and able to communicate with each other and execute the workflow without the UI).

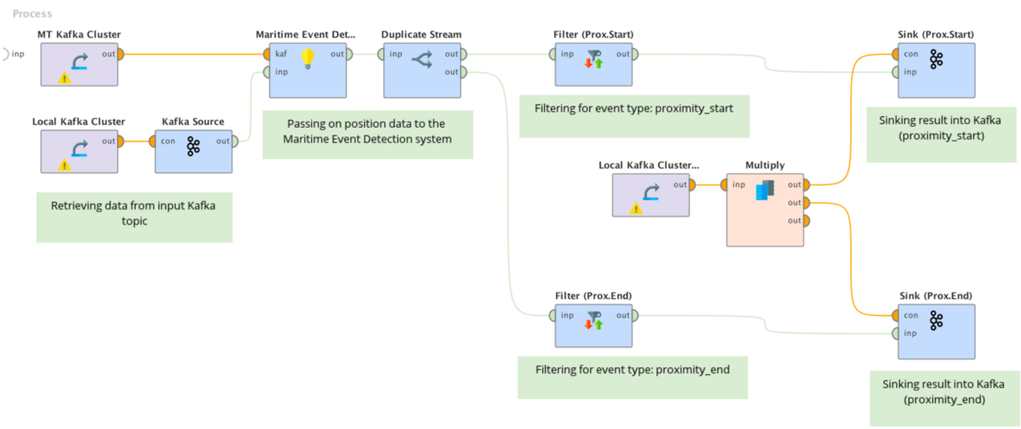

Figure 42: Workflow 1

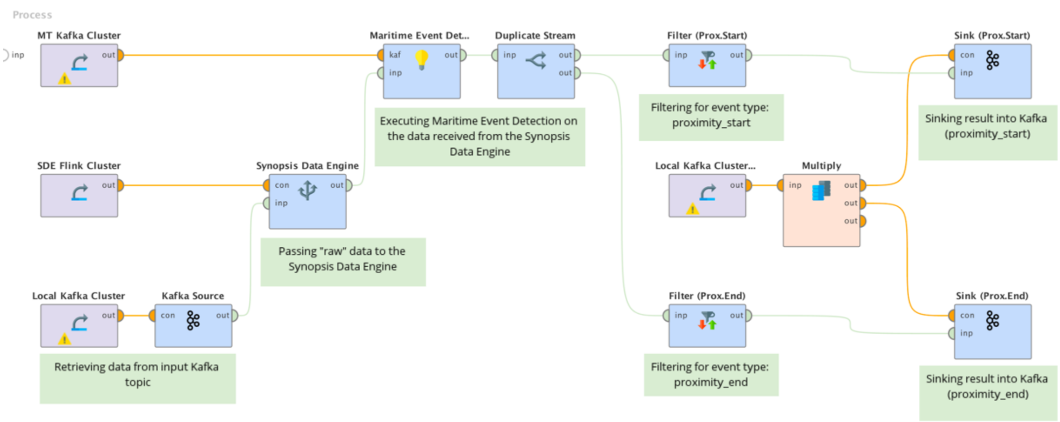

Figure 43: Workflow 2

6 Next phase: the pilot experiment at sea

In this section we report the initial planning of the pilot experiment in which the single use case components, for local and global view, will be integrated into the maritime situational awareness platform and demonstrated at sea.

In general, the pilot experiment will be tailored for an application of border and harbour protection and littoral area surveillance for which a hybrid sensor network will be deployed for the detection, localization and classification of suspect maritime targets. Specific goals of the experiment are the comparison of cooperative vs non-cooperative sensor network and the improvement in situational awareness KPIs (see section 2.2) by integrating global view provided by AIS and satellite with local view from the hybrid sensor network.

The main reasons for having an experiment at sea is to test a cooperative sensor network on site to push the roadmap for highly innovative robotic maritime surveillance systems, demonstrate how the INFORE architecture can handle distributed sensor nodes, acquire real data to refine coordination and classification algorithms and improve the use case component performance and hence that of the whole system, and finally to cope with issues that can be experienced only in a true at sea experiment rather than in a simulated one, like imperfect communication between the network nodes and non-ideal robot dynamic coupled with environmental conditions.

This section will describe the pilot experiment including possible location, involved assets, the data that will be acquired and the scenario to test.

The possible location of the pilot is depicted in Figure 44. The area is positioned in the Ligurian Sea close to the Palmaria Island, Italy. The autonomous wave gliders will be deployed in the rectangular area depicted on the right in blue while a thermal camera and a RGB camera will observe the area of interest from a site on the island. A Command and Control (depicted in red) centre is positioned on Palmaria Island, as well, to receive and fuse the data from the wave gliders and the cameras, and send target contact positions, vehicle data and target classification labels to the remote situational awareness platform that integrates the global and local views and performs high level target behavioural analysis.

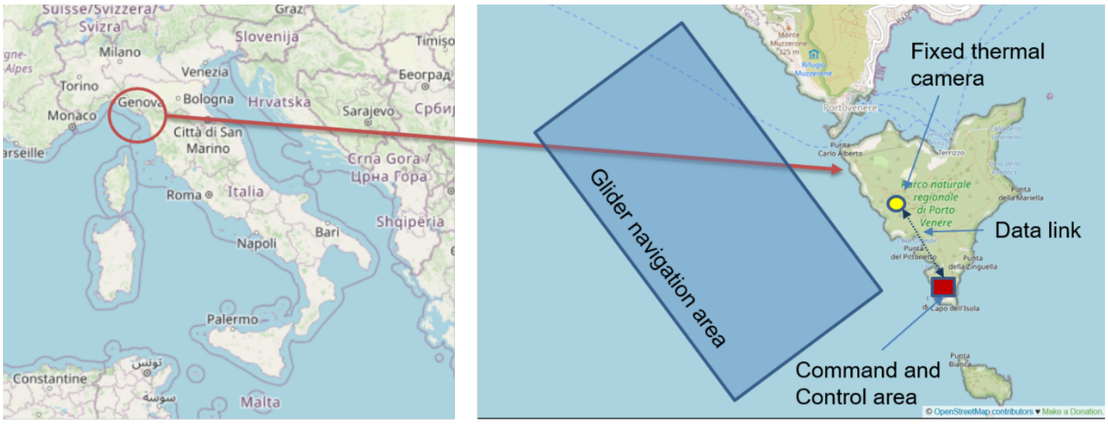

Figure 44: Possible area of the pilot experiment.

The experiment assets will include a coordinated sensor network of two autonomous wave-gliders with acoustic passive sensors on board for surface target detection and localization, one on shore thermal camera and a co-located RGB video camera, and, possibly, one reactive and rapid vehicle (a rubber boat) with optical camera for suspect target inspection. The target is simulated by using a second rubber boat equipped with an AIS transmitter and a GPS for position and speed ground truth.

The experiment operations can be summarised as follows (see Figure 45): the test target, in red, enters the pilot area and performs a scenario. Surveillance assets cooperate to monitor the pilot area and acquire data that will be fused to detect, localize and classify the target. The target information is transmitted to the remote situational awareness platform where the target behaviour is analysed and an alert is generated in case an anomalous behaviour is detected. The alarm is feed backed to the field to trigger the fast reactive boat which navigates to intercept and inspect the target.

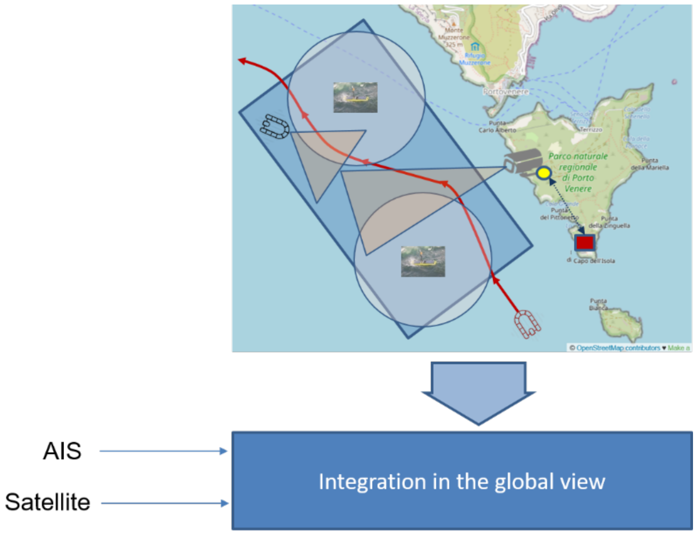

Figure 45: Operations during the pilot experiment.

During the experiment, five scenarios will be tested (see Figure 46). The first one consists in detecting a dark target that switched off the AIS transponder to hide its position. In the second scenario, a denied area is monitored and an alert is generated every time a target is detected while entering the area. The third scenario consists in simulating a vessel trajectory spoofing, i.e. a vessel declare a different position with respect to the actual one. The fourth test will be conducted by simulating a vessel which exhibits an irregular behaviour with respect to the normal one which is expected in the area. In the final scenario, the interaction between two vessels engaged in an illegal transfer will be simulated.

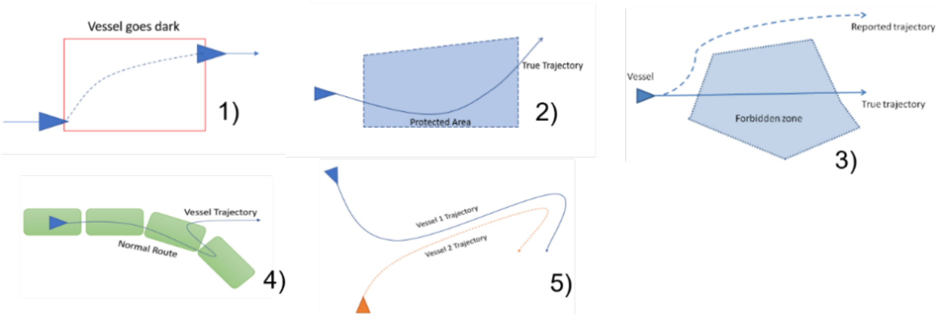

Figure 46: Use case scenario to test during the pilot experiment.

The local view data that will be acquired during the experiment include:

- Target position, ground truth and estimated
- Acoustic raw data
- Target bearing angle measurements
- Wave-gliders positions & attitude
- Target presence probability map
- Target classification scores and labels
- Thermal camera and RGB camera raw data

The data sets will be made available to the Project INFORE partners.

Figure 47 shows a preliminary plan of the pilot experiment. In consists of two phases. The first one is preliminary to the actual test trial and includes one day to bring the material from CMRE on site and start the installation of the experiment setup, a second day in which the setup is finalized and the vehicles, sensors and communication are tested, and a third day in which to finalize the component tests and start to test some scenario execution. In the second part of the pilot, three days long, the scenarios from 1 to 5 are executed and the data are acquired. In the final day, the experiment setup is dismantled and the material brought back to CMRE.

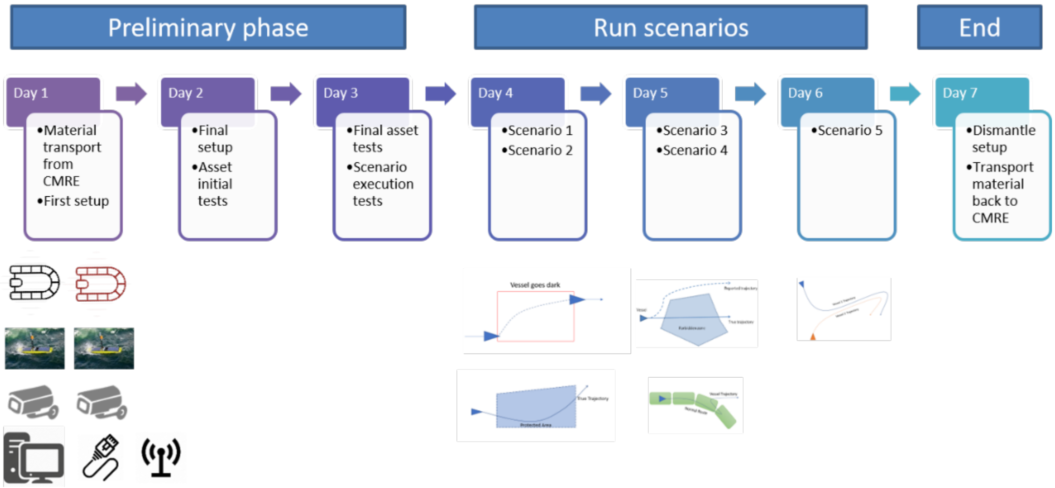

Figure 47: Pilot experiment plan. The preliminary phase includes logistic, first setup and testing of assets and scenarios. In the second phase the scenario from 1 to 5 will be executed. The trail will end with setup dismantle and transport back of the material to CMRE

7 Expert evaluation

Four Experts from MarineTraffic were interviewed in order to evaluate the results described in this deliverable. Due to the COVID-19 situation, the evaluation was performed remotely and the experts completed a questionnaire via the EU-Survey platform. The anonymized results of the questionnaires are provided in Appendix-III.

8 Conclusions

This work reports the result of the preliminary evaluation of the Maritime Use Case hybrid sensor network and situational awareness system that will be deployed and evaluated during the final Project pilot experiment at sea.

In particular, the algorithms for target detection, localization and classification that will process the single sensor data streams perform in line with the expectations, although some space for further improvement is expected. The robotic adaptive sensor network, when tested on simulated scenarios, outperforms the base model system having no coordination algorithm. Classification algorithms for satellite data and camera data performs well with classification accuracy in general greater than 90% on train, validation and test data sets. The first implementation of the classification of vessel activities as complex events using machine learning techniques is currently deployed in the MarineTraffic infrastructure and is constantly tested and evaluated.

The report also provides a preliminary plan for the experimentation at sea in which we selected involved assets, we proposed a possible location of the experiment and the configuration of the field command and control centre that will be interfaced with the high-level data fusion situational awareness system. Moreover, we chose 5 scenarios to be simulated during the experiment to evaluate the Maritime Use Case which are representative of a harbour/border protection and denied area surveillance application.

Future work on the robotic coordinated sensor network includes the implementation of the target detection and localization algorithm on board the wave-glider vehicles and of the coordination and control software.

Further tests will be conducted on the target classification algorithms for satellite and camera data including experiments on new data sets and new deep learning architectures.

In the future, we plan to make use of the whole INFORE Architecture to tackle the maritime situational awareness use case. Thereby the Graphical Editor component is used to easily design analysis workflows, which are executed on the large-scale data stream of the hybrid sensor network. Specific operators are designed in cooperation with RapidMiner to include the event detection functionality in the designed workflows. In addition the Online Machine Learning component is extended in collaboration with ATHENA in order to implement online versions of the RF algorithm, enabling us to automatically label new, detected maritime events on real-time streams and at the same time update our model, increasing the overall accuracy incrementally.

Finally, a simulated test on the integrated use case system will be conducted before the experiment at sea for which the design of a detailed plan, including logistic aspects, will start soon this year.

References

[1] Ferri, G., Bates, J., Stinco, P., Tesei, A., and LePage, K., (2018). Autonomous underwater surveillance networks: a task allocation framework to manage cooperation. In OCEANS 2018, Kobe (Japan).

[2] Ferri, G., Tesei, A., Stinco, P., and LePage, K. D., June 2019. A Bayesian Occupancy Grid Mapping Method for the Control of Passive Sonar Robotics Surveillance Networks. In OCEANS 2019 - Marseille, pp. 1–9.

[3] Elfes, A. Occupancy grid: a probabilistic framework for robot perception and navigation. PhD thesis, Department of Electrical and Computer Engineering, Carnegie Mellon University, (1989).

[4] Thrun, S., Burgard, W., and Fox, D., (2005). Probabilistic robotics. The MIT Press.

[5] Jungnickel, R., Khler, M., and Korf, F., June 2016. Efficient automotive grid maps using a sensor ray based refinement process. In 2016 IEEE Intelligent Vehicles Symposium (IV), pp. 668–675.

[6] Jakuba, M. Stochastic mapping for chemical plume source localization with application to hydrothermal vent discovery. PhD thesis, WHOI-MIT, (2007).

[7] Ferri, G., Jakuba, M., Mondini, A., Mattoli, V., Mazzolai, B., Yoerger, D., and Dario, P., (2011). Mapping multiple gas/odor sources in an uncontrolled indoor environment using a Bayesian occupancy grid mapping based method. Robotics and Autonomous Systems 59 (11), pp. 968–1000.

[8] Jakuba, M. and Yoerger, D., (2008). Autonomous search for hydrothermal vent fields with Occupancy Grid Maps. In Proceedings of the 2008 Australasian Conference on Robotics & Automation.

[9] Milstein, A., (2008). Occupancy Grid Maps for Localization and Mapping. Motion Planning Xing-Jian Jing, IntechOpen.

[10] Meyer-Delius, D., Beinhofer, M., and Burgard, W., (2012). Occupancy Grid Models for Robot Mapping in Changing Environments. In Proceedings of The Twenty-Sixth AAAI Conference on Artificial Intelligence.

[11] Ferri, G. and Tesei, A. Autonomous strategies for passive acoustic monitoring. Technical report, CMRE-MR-2018, (2018).

[12] Wagner, D., Mylander, W., and Sanders, T., (1999). Naval Operations Analysis.

[13] Hoffmann, G. M. and Tomlin, C. J., Jan 2010. Mobile Sensor Network Control Using Mutual Information Methods and Particle Filters. IEEE Transactions on Automatic Control, 55(1), 32–47.

[14] Martinez, S. and Bullo, F., April 2006. Optimal Sensor Placement and Motion Coordination for Target Tracking. Automatica, 42(4), 661–668.

[15] Hero, A. O. and Cochran, D., (2011). Sensor management: past, present, and future. IEEE Sensors Journal, 11, Issue 12, 3064–3075.

[16] Stachniss, C., Grisetti, G., and Burgard, W., (2005). Information gain-based exploration using Rao-Blackwellized particle filters. In RSS 2005.

[17] I. Goodfellow, Y. Bengio, and A. Courville, Deep Learning. The MIT Press, 2016.

[18] Bishop, Christopher M., Pattern Recognition and Machine Learning, Springer, 2006.

[19] Armin Haller, Krzysztof Janowicz, Simon Cox, Maxime Lefran ̧cois, Kerry Taylor, Danh Le Phuoc, Josh Lieberman, Raùll Garcìa-Castro, Rob Atkinson, and Claus Stadler. The modular ssn ontology: A joint W3C and OGC standard specifying the semantics of sensors, observations, sampling, and actuation. Semantic Web Journal, 2018.

[20] Tarek Elsaleh, Shirin Enshaeifar, Roonak Rezvani,Sahr Thomas Acton, Valentinas Janeiko, and Maria Bermudez-Edo. IoT-Stream: A Lightweight Ontology for Internet of Things Data Streams and Its Use with Data Analytics and Event Detection Services. Sensors (Basel) 20(4):953, 2020 Feb, doi: 10.3390/s20040953

[21] Mark van Assem Hajo Rijgersberg and Jan Top. Ontology of units of measure and related concepts. Semantic Web Journal, 2011.

[22] Shashi K. Gadia. The role of temporal elements in temporal databases. IEEE Data Eng. Bull., 11(4):19–25, 1988.

[23] Joint Committee for Guides in Metrology (JCGM/WG 1). Evaluation of measurement data — guide to the expression of uncertainty in measure- ment.

[24] Marna Riga, Efstratios Kontopoulos, Konstantinos Ioannidis, Spyridon Kintzios, Stefanos Vrochidis, and Ioannis Kompatsiaris. Eucise-owl: An ontology-based representation of the common information sharing environment (CISE) for the maritime domain. Semantic Web Journal, 2019.

[25] Willem Robert van Hage, Véronique Malaisé, Roxane Segers, Laura Hollink, and Guus Schreiber. Design and use of the simple event model (sem). 2011.

[26] Adila A. Krisnadhi and Pascal Hitzler. A core pattern for events. In Proceedings of the 7th Workshop on Ontology and Semantic Web Patterns (WOP2016) (ISWC2016 workshop), October 18, 2016, Kobe, Japan, 2016.

[27] Jean Roy and Michael Davenport. Categorization of Maritime Anoma- lies for Notification and Alerting Purpose. Technical Report DRDC-VALCARTIER-SL-2009-394, Defence R&D Canada, September 2009.

[28] Cyril Ray, Anne-Laure Jousselme, Clément Iphar, Maximilian Zocholl, Elena Camossi, Richard Dréo. (2020) Mobility Data: A Perspective from the Maritime Domain. In: Vouros G. et al. (eds) Big Data Analytics for Time-Critical Mobility Forecasting. Springer, Cham. https://doi.org/10.1007/978-3-030-45164-6_1

[29] Manolis Pitsikalis, Alexander Artikis, Richard Dréo, Cyril Ray, Elena Camossi, Anne Laure Jousselme. Composite Event Recognition for Maritime Monitoring. DEBS '19: Proceedings of the 13th ACM International Conference on Distributed and Event-based SystemsJune 2019 Pages 163–174 https://doi.org/10.1145/3328905.3329762

[30] Maria Nilsson, Joeri van Laere, Tom Ziemke, and Johan Edlund. Extract- ing rules from expert operators to support situation awareness in maritime surveillance. In Proceedings of the 11th International Conference on Infor- mation Fusion, FUSION 2008, pages 908–915, 2008.

[31] ITU, "Technical characteristics for an automatic identification system using time division multiple access in the vhf maritime mobile band," International Telecommunications Union, Tech. Rep. ITU-R M.1371-5, 02 2014.

[32] "ESA-Sentinel-2 mission website," https://sentinel.esa.int/web/sentinel/missions/sentinel-2, accessed: 2018-12-07.

[33] "ESA-Sentinel-2 mission website," https://earth.esa.int/web/sentinel/user-guides/sentinel-2-msi/resolutions/radiometric, accessed: 2018-12-07.

[34] "Copernicus Science Hub website," https://scihub.copernicus.eu, accessed: 2018-12-07.

[35] Joseph Redmon, Santosh Kumar Divvala, Ross B. Girshick, Ali Farhadi: You Only Look Once: Unified, Real-Time Object Detection. CVPR 2016: 779-788

[36] T.-Y. Lin, M. Maire, S. Belongie, J. Hays, P. Perona, D. Ramanan, P. Dollar, and C. L. Zitnick. Microsoft coco: Com- ´ mon objects in context. In European conference on computer vision, pages 740–755. Springer, 2014.

[37] Oleh Bodunov, Florian Schmidt, André Martin, Andrey Brito, and Christof Fetzer. 2018. Real-Time Destination and ETA Prediction for Maritime Traffic. In Proceedings of the 12th ACM International Conference on Distributed and Event-Based Systems (Hamilton, New Zealand) (DEBS .ĂŹ18). Association for Computing Machinery, New York, NY, USA,

[38] Konstantinos Chatzikokolakis, Dimitrios Zissis, Giannis Spiliopoulos, and Konstantinos Tserpes. 2018. Mining Vessel Trajectory Data for Patterns of Search and Rescue. In EDBT/ICDT Workshops.

[39] Richard Duda, Peter Hart, and David G. Stork. 2001. Pattern Classification. Vol. xx

[40] Vaughn Vernon. 2015. Reactive Messaging Patterns with the Actor Model: Applications and Integration in Scala and Akka (1st ed.). Addison-Wesley Professional.

[41] Liquid Robotics web site: https://www.liquid-robotics.com/wave-glider/overview/

[42] Dimitris Zissis, Konstantinos Chatzikokolakis, Giannis Spiliopoulos and Marios Vodas, "A distributed spatial method for modeling maritime routes", in IEEE Access.

[43] Ioannis Kontopoulos, Konstantinos Chatzikokolakis, Konstantinos Tserpes, Dimitris Zissis. Classification of vessel activity in streaming data. DEBS 2020.

[44] Konstantina Bereta, Raffaele Grasso, Dimitris Zissis. Vessel detection using image processing and Neural Networks. IGARSS 2020 (to appear).

[45] Konstantina Bereta, Raffaele Grasso, Dimitris Zissis. Automatic Maritime Object Detection Using Satellite imagery. IEEE OCEANS 2020 (extended abstract accepted).

[46] Aristides Milios, Konstantina Bereta, Konstantinos Chatzikokolakis, Dimitris Zissis, Stan Matwin: Automatic Fusion of Satellite Imagery and AIS data for Vessel Detection. FUSION 2019: 1-5

[47] Kaiming He, Xiangyu Zhang, Shaoqing Ren, Jian Sun: Deep Residual Learning for Image Recognition. CVPR 2016: 770-778

[48] Bart Lariviere and Dirk Van den Poel. 2005. Predicting Customer Retention and Profitability by Using Random Forests and Regression Forests Techniques. Expert Systems with Applications 29 (08 2005), 472–484.

Appendix I- Detailed description of data sources

AIS data. AIS messages are distinguished on the following two categories:
(i) dynamic, and (ii) static. Dynamic messages contain positional data about voyages. Static messages contain information related to vessel characteristics. The information (e.g., flag)
changes less frequently than the respective information included in static messages.
The fields of dynamic AIS messages is described as follows:

- The *Maritime Mobile Service Identity Number* (MMSI)}. The MMSI is an identification number for each vessel station.
- *Rate of Turn*. This field contains data regarding the angle that the vessel turns right or left per minute. The values of this field range from 0 to 720 degrees.
- *Speed over Ground*. Speed over ground is the speed of the ship with respect to the ground. The value range of this attribute is from 0 to 102 knots (0.1-knot resolution).
- *Position Coordinates*. This field contains the latitude and the longitude of the position of the vessel.
- *Course over Ground (COG)*. COG describes the direction of motion with respect to the ground that a vessel has moved relative to the magnetic north pole or geographic north pole. The values are degrees up to 0.1 degrees relative to true north.
- *Heading*. Heading describes the direction that a vessel is pointed at any time relative to the magnetic north pole or geographic north pole. Heading takes values from 0 to 359 degrees.
- *UTC seconds*. This is the second part of the timestamp when the subject data-packet was generated (in UTC time).
- AIS Navigational status. This field represents the navigational status of the vessel and it is completed manually by the crew. The different types of navigational status that can be reported in an AIS message are the following:
    - *Under way using engine*: the vessel is travelling using its engine.
    - *Anchored*: The vessel is not travelling and has dropped an anchor.
    - *Not under command*: The vessel is un-commanded. This can be either due to a hardware malfunction or a problem of the crew (e.g., the commander is injured).
    - *Restricted maneuverability*: There are constraints regarding the motion of the vessel (e.g., tugging heavy load).
    - *Constrained by her draught*: The draught (or draft) of a vessel is the vertical distance between the waterline and the bottom of the hull (keel). The draught is an indicator that shows how much a vessel is loaded. So, a vessel carrying heavy load might have maneuverability restrictions (e.g., navigating in shallow waters).
    - *Moored*: The vessel is moored at a fixed point (e.g., dock).
    - *Aground*: The vessel is touching the ground, after navigating in shallow water.
    - *Engaged in fishing activity*: The vessel is currently fishing.
    - *Underway sailing*: The vessel is travelling using sails instead of engine (it applies to sailing vessels).

The static AIS messages contain the following fields:

- The International Maritime Organisation number (IMO)}. This is a 9-digit number that uniquely identifies the vessel. Please note that this is not the same as the MMSI. The IMO number is assigned by IHS Maritime (Information Handling Services) when the vessel was constructed[12]}. The MMSI can change, for example when the owner changes. Only propelled, seagoing vessels of 100 gross tons and above are assigned an IMO number.
- Call Sign. The international radio call sign assigned to the vessel by her country of registry.
- Name. The name of the vessel.
- Type. The type of the vessel (e.g., Tanker).
- Dimensions. Dimensions of ship in meters. More specifically, this field refers to:

(a) dimension to bow, (b) dimension to stern, (c) dimension to port (left side of the vessel when facing the bow), and (d) dimension to starboard (i.e., right side of the vessel when facing the bow).

- Location of the positioning system's antenna on-board the vessel.
- Type of positioning system (GPS, DGPS, Loran-C.

[12] https://ihsmarkit.com/products/imo-ship-company.html}

- Draught. The term draught (or draft) refers to the vertical distance between the waterline and the bottom of the hull (keel), with the thickness of the hull included. The value of this field is measured in meters.
- Destination. The destination as completed manually by the crew of the subject vessel (free text).
- Estimated time of arrival (ETA). This is a UTC timestamp completed manually by the crew indicating the estimated time of arrival at destination.

A sample of this dataset is also published in Zenodo[13].

Satellite data. We use satellite images provided by the European Space Agency (ESA) Copernicus data Hub[14] acquired from the Sentinel-1 and Sentinel-2 satellites. Sentinel-1 provides radar images, as it is equipped with a C band multi-polarized SAR sensor operating at four different modes: strip map, interferometric wide swath, extra wide swath and wave mode. Each operational mode is characterized by its own viewing geometry resolution and polarization channels (named HH, VV, VH and HV channels). The Ground Range Detected (GRD) Level 1 data product is one of the possible formats that will be utilized in the maritime use case. The product is provided for the channels VH and VV. For each channel the data are stored in a GeoTIFF format file on a grid with a pixel spacing of 10x10m. The size of the grid is variable depending on the acquisition and of the order of ten thousands of pixels in each direction. Metadata files in XML format are associated to each grid to provide, so that it can be used for georeferencing.

The Sentinel-2 pair of satellites are equipped with a multi-spectral instrument (MSI) for acquiring the solar radiation from the Earth surface and the atmosphere in 13 spectral bands (or channels) at three different resolutions: four bands have a resolution of 10 meters/pixel, six bands at 20 meters/pixel and three bands at 60 meters/pixel spatial resolution. For the L1C product level, the image data of each band is provided as a geo-located regular grid (in UTM coordinates) in JP2000 uncompressed format on 16 bits, with auxiliary XML metadata files which include information such as the geo-localization grid parameters, the satellite ephemerides, the acquisition time, applied post-processing procedures if any, calibration coefficients and quality check The image grid size depends on the channel resolution; at 10m of resolution, for instance, the image size is 10800x10800 samples. Using the GDAL library, we convert the JP2000 format of Sentinel-2 images into GeoTIFF.

Acoustic data.
The acoustic data are acquired by arrays of passive hydrophones towed by autonomous surface vehicles to detect, localize and classify targets of interest. The acoustic data are processed on board the vehicles to extract target bearing and associated uncertainty data. The bearing and the bearing uncertainty for each detected target, together with the position of the vehicles, are continuously exchanged between vehicles and a fusion centre for further processing. The vehicles also exchange some results from a first target classification based on the acoustic data. The produced bearing measurements are the input on one side to cooperative target localization behaviours running on the vehicles, on the other are used at a fusion centre to compute the probabilities of the presence of targets in the monitored area. This processed information can provide hints to the thermal camera data on specific areas of interest to be further imaged. Furthermore, this information can be fused with the output of the thermal camera data for target confirmation and classification.

Thermal camera data.
Thermal video camera data will be acquired for target detection and classification in a spectral range between 3.6 and 4.9 μm using a 640x480 pixel Indium Antimonide (InSb) Focal Plane Array (FPA) detector. The camera is able to provide a continuous composite video PAL or NTSC stream which can be converted in a digital stream (e.g. MPEG4 or AVI) for further processing including automatic target detection and classification.

[13] https://zenodo.org/record/3754481#.XtqGaJ4zYkg

[14] https://scihub.copernicus.eu/

Appendix II-Target detection and localization message format.

This Appendix describes measurement xml that is transmitted by the Topside to the INFORE system. The message is composed by assembling robot positions and measurements running the target estimation algorithm and producing a target position estimate to be sent to the INFORE system.

The message is an XML one and is produced every Updated Time (that can be selected, indicatively every 1 minute), with the latest produced information.

In the following a detailed description of the format with comments inline to describe the relative field. Robot_info and alarm_elements are repeated for each vehicle of the network.

<time>xxx</time>			/*epoch in ms. It is the last used data for estimating the target used by the Topside
<robot_info>			/* information regarding the vehicles / we can have multiple tag
	<id>xxx</id>		/*unique ID of the vehicle
	<type>xxx</type>		/*vehicle type (e.g. waveglider)
	<sensor_model>xxx</sensor_model>		/*sensor model (e.g. PERSEUS MOD1)
	<robot_position>		
		<time>xxx</time>	/*epoch in ms. Time of the last received robot position update
		<lat>yyy</lat>	/*double – WGS84
		<lon>xxx</lon>	/*double – WGS84
		<heading>hhh</heading>	/*[0-360] degree – compass convention
		<speed>sss</speed>	/*[m/s]
	</robot_position>		
</robot_info>			
<target_position>			/*estimated target position using data fusion
	<lat>yyy</lat>		/*double – WGS84
	<lon>xxx</lon>		/*double – WGS84
	<quality_index>pppp</quality_index>		/* quality of the detection (fused map occupancy probability) [0-1]
	<uncertainty_measure>uuuu</uncertainty_measure>		/* a measure of the target localization accuracy [m]
</target_position>			
<alarm>			/*Each alarm refers to 1 veichle identified by the id; all the alarms encountered during the update period are reported
	<id>xxx</id>		/*unique ID of the vehicle
	<alarm_code1>aaa</alarm_code1>		/*integer>0 see the alarm code table
	<alarm_code2>bbb</alarm_code2>		/*integer>0 see the alarm code table
</alarm>			

Appendix III-Expert questionnaires

This appendix provides the anonymized questionnaires of the 4 experts interviewed by MarineTraffic.

Existing MSA workflows

Please describe the different kinds of data sources that you use in your day-to-day tasks and the tools that you use to process them

AIS data, RADAR data, camera data, and satellite data are the main sources of data that I use. I use a wide variety of tools such as Panoply, GNU Radio companion, Eumetcast View, SDR, SDR Console v3.

How many tools do you typically use to integrate or handle the different sources of data mentioned above

5

What are the events you are trying to identify?

- [x] fishing
- [ ] piloting
- [ ] smuggling
- [ ] trafficking
- [ ] transshipments
- [ ] tugging

Any additional events you would like to identify?

dark targets, drifting, STS

What data processing challenges do you experience in your day-to-day tasks (e.g., fusion of heterogeneous sources, performance, analytics)? Rate them starting from 1 (lowest priority) to 5 (highest priority).

Please use each priority number only once

	1	2	3	4	5
Streaming nature of data	○	●	○	○	○
Too much data	○	○	●	○	○
Different data formats	○	○	○	○	●
Manual workflows	○	○	○	●	○

Any additional challenges?

Please complete challenges that are not mentioned above (optional).

fusion of data from different sources

Do you write code to automate the data analysis process?

- (●) Yes
- ( ) No

Do you program/set up a new/custom data processing workflows?

- (x) Yes
- ( ) No

How long does it take to set up such a process?

It could take up to a month.

Can you optimise your data analysis operations?

Yes, a lot of effort is directed towards optimisation operations.

On what kind of infrastructure(s) do you usually run the analysis:

- [ ] cluster
- [x] high spec workstation
- [ ] HPC
- [x] personal laptop
- [ ] server

INFORE solutions

Which INFORE data sources would be useful for you for the MSA Use Case and would be useful for you:

- [x] Acoustic data
- [x] AIS data
- [x] Satellite imagery
- [x] Thermal Camera data

Other data sources?

Which events would you like to extract from these data sources?

- [x] Normal vessel activities (fishing, transshipments, tugging, piloting, etc.)
- [x] Illegal vessel activities (smuggling, illegal fishing, entering protected/prohibited areas, etc.)
- [x] Other

Other events?

Please complete any other events that are not mentioned above and you would like to detect/forecast.

AIS off

Rate your satisfaction on the variety of maritime complex events that INFORE is able to forecast, accuracy and interpretability of results:

	1: Not at all	2: Very little	3: Neutral	4: Pretty much	5: Very much
How much are you satisfied by the variety of complex events that can be forecasted?	○	○	○	○	●
How much would you trust the output of the INFORE platform with respect to accuracy?	○	○	○	●	○
To what extent do you understand the results presented to you?	○	○	○	●	○

Are there specific events that you would like to forecast in real-time, which we currently cannot forecast? If so, please explain.

If the answer is "No", you can leave this field blank.

Rate the following objectives of INFORE, based on how useful they are at YOUR data analysis.

	1: Not useful	2: Little Use	3: Average Use	4: Quite useful	5: Very useful
Ability to design data processing workflows with no code required	○	○	●	○	○
Ability to change algorithm parameters graphically	○	○	●	○	○
Ability to receive quick approximate answers instead of 100% accurate, but long running queries	○	○	○	○	●
Ability to interactively explore the data in order to detect patterns/features of interest	○	○	○	●	○
Ability to accurately forecast events of interest	○	●	○	○	○
over different data processing platforms (HPC, Big Data Platforms, etc).	○	●	○	○	○

What is the expected added value from INFORE for you and your corporation. Rate from 1 (lowest priority) to 5 (highest priority).

You can assign each number to multiple options.

	1	2	3	4	5
Performance	○	○	○	●	○
Ability to handle multiple sources	○	○	○	○	●
Timely forecast of events	○	○	○	●	○
Interactive and efficient optimizable workflows will save time and improve	○	○	●	○	○

Automation of processes will reduce human error	○	●	○	○	○

Overall evaluation

How likely would your organisation be to use the INFORE platform operationally in the future?	★★★★☆
How useful is the combination of data sources used in INFORE?	★★★★★

☑ I have read and understood the information sheet, or it has been read to me. I have been given the opportunity and enough time to ask questions about the study and my questions have been fully answered.I agree voluntarily to be a participant in this study and understand that I can decide to withdraw from the study at any time.I understand that taking part in the study may involve audio-recorded interviews and I am willing to devote enough time to respond to the questionnaire.I give permission for the data that I provide to be de-identified and deposited in a repository so it can be used for INFORE's purposes as outlined above.I understand that personal information collected about me, will not be shared and only de-identified or aggregative information will be used for INFORE purposes.I understand that de-identified or aggregative information I provide may be used for reports and research outputs, possibly made available to websites and social media.

Terms and privacy policy

Responses you give in the questionnaires and interviews may be recorded. Your recorded data will be de-identified; hence it will not be possible to identify your identity afterwards. Information will be processed during the phase of requirement analysis and aggregative results may be presented in project reports. It will not be possible to identify the individual source (that is you) of the information. The aggregative results of this investigation may be published in scientific journals or conferences and may be used in further studies. No personal data will be handed out to third parties.You can request your information be deleted at any time, without giving a reason. If you should decide to deny your consent, please contact the Project Coordinator, Prof. Antonios Deligiannakis (adeli[at]imin.athena-innovation.gr) and let him know of your intention of leaving the study.Your participation in this study is only possible if you freely and independently agree to authorize the INFORE consortium to use the data you provide. With your consent, the data will be stored for the purposes described above until the end of the project (31/12/2021), when all data will be permanently deleted .

☑ I accept the terms and privacy policy described above.

Contact

konstantina.bereta@marinetraffic.com

Existing MSA workflows

Please describe the different kinds of data sources that you use in your day-to-day tasks and the tools that you use to process them

> mainly MarineTraffic AIS data, mainly python and postgresql

How many tools do you typically use to integrate or handle the different sources of data mentioned above

> 2-3

What are the events you are trying to identify?

- [ ] fishing
- [ ] piloting
- [x] smuggling
- [ ] trafficking
- [x] transshipments
- [x] tugging

Any additional events you would like to identify?

> run aground vessels, laid up vessels, distress due to weather conditions, piracy events

What data processing challenges do you experience in your day-to-day tasks (e.g., fusion of heterogeneous sources, performance, analytics)? Rate them starting from 1 (lowest priority) to 5 (highest priority).

Please use each priority number only once

	1	2	3	4	5
Streaming nature of data		[x]			
Too much data				[x]	
Different data formats			[x]		
Manual workflows					[x]

Any additional challenges?

Please complete challenges that are not mentioned above (optional).

>

Do you write code to automate the data analysis process?

- [x] Yes
- [ ] No

Do you program/set up a new/custom data processing workflows?

- [x] Yes
- [ ] No

How long does it take to set up such a process?

a few months

Can you optimise your data analysis operations?

yes

On what kind of infrastructure(s) do you usually run the analysis:

- [ ] cluster
- [x] high spec workstation
- [ ] HPC
- [ ] personal laptop
- [x] server

INFORE solutions

Which INFORE data sources would be useful for you for the MSA Use Case and would be useful for you:

- [x] Acoustic data
- [ ] AIS data
- [x] Satellite imagery
- [x] Thermal Camera data

Other data sources?

bathymetry data, shipping lanes data

Which events would you like to extract from these data sources?

- [ ] Normal vessel activities (fishing, transshipments, tugging, piloting, etc.)
- [x] Illegal vessel activities (smuggling, illegal fishing, entering protected/prohibited areas, etc.)
- [ ] Other

Rate your satisfaction on the variety of maritime complex events that INFORE is able to forecast, accuracy and interpretability of results:

	1: Not at all	2: Very little	3: Neutral	4: Pretty much	5: Very much
How much are you satisfied by the variety of complex events that can be forecasted?	○	○	○	■	○
How much would you trust the output of the INFORE platform with respect to accuracy?	○	○	○	■	○

To what extent do you understand the results presented to you?	○	○	○	○	●

Are there specific events that you would like to forecast in real-time, which we currently cannot forecast? If so, please explain.

If the answer is "No", you can leave this field blank.

run aground vessels, laid up vessels, distress due to weather conditions, piracy events

Rate the following objectives of INFORE, based on how useful they are at YOUR data analysis.

	1: Not useful	2: Little Use	3: Average Use	4: Quite useful	5: Very useful
Ability to design data processing workflows with no code required	○	○	○	●	○
Ability to change algorithm parameters graphically	○	○	●	○	○
Ability to receive quick approximate answers instead of 100% accurate, but long running queries	○	○	●	○	○
Ability to interactively explore the data in order to detect patterns/features of interest	○	○	○	○	●
Ability to accurately forecast events of interest	○	○	○	○	●
over different data processing platforms (HPC, Big Data Platforms, etc).	○	○	○	●	○

What is the expected added value from INFORE for you and your corporation. Rate from 1 (lowest priority) to 5 (highest priority).

You can assign each number to multiple options.

	1	2	3	4	5
Performance	○	○	●	○	○
Ability to handle multiple sources	○	○	●	○	○
Timely forecast of events	○	○	○	○	●
Interactive and efficient optimizable workflows will save time and improve	○	○	○	○	●
Automation of processes will reduce human error	○	○	○	●	○

Overall evaluation

How likely would your organisation be to use the INFORE platform operationally in the future?	★★★★☆

How useful is the combination of data sources used in INFORE?	★★★★★

☑ I have read and understood the information sheet, or it has been read to me. I have been given the opportunity and enough time to ask questions about the study and my questions have been fully answered.I agree voluntarily to be a participant in this study and understand that I can decide to withdraw from the study at any time.I understand that taking part in the study may involve audio-recorded interviews and I am willing to devote enough time to respond to the questionnaire.I give permission for the data that I provide to be de-identified and deposited in a repository so it can be used for INFORE's purposes as outlined above.I understand that personal information collected about me, will not be shared and only de-identified or aggregative information will be used for INFORE purposes.I understand that de-identified or aggregative information I provide may be used for reports and research outputs, possibly made available to websites and social media.

Terms and privacy policy

Responses you give in the questionnaires and interviews may be recorded. Your recorded data will be de-identified; hence it will not be possible to identify your identity afterwards. Information will be processed during the phase of requirement analysis and aggregative results may be presented in project reports. It will not be possible to identify the individual source (that is you) of the information. The aggregative results of this investigation may be published in scientific journals or conferences and may be used in further studies. No personal data will be handed out to third parties.You can request your information be deleted at any time, without giving a reason. If you should decide to deny your consent, please contact the Project Coordinator, Prof. Antonios Deligiannakis (adeli[at]imin.athena-innovation.gr) and let him know of your intention of leaving the study.Your participation in this study is only possible if you freely and independently agree to authorize the INFORE consortium to use the data you provide. With your consent, the data will be stored for the purposes described above until the end of the project (31/12/2021), when all data will be permanently deleted .

☑ I accept the terms and privacy policy described above.

Contact

konstantina.bereta@marinetraffic.com

Existing MSA workflows

Please describe the different kinds of data sources that you use in your day-to-day tasks and the tools that you use to process them

MS DB data, data from external sources like csv, python, mssql, orange3

How many tools do you typically use to integrate or handle the different sources of data mentioned above

about 3 tools

What are the events you are trying to identify?

- [ ] fishing
- [ ] piloting
- [x] smuggling
- [x] trafficking
- [x] transshipments
- [ ] tugging

Any additional events you would like to identify?

What data processing challenges do you experience in your day-to-day tasks (e.g., fusion of heterogeneous sources, performance, analytics)? Rate them starting from 1 (lowest priority) to 5 (highest priority).

Please use each priority number only once

	1	2	3	4	5
Streaming nature of data	●	○	○	○	○
Too much data	○	○	○	○	●
Different data formats	○	○	●	○	○
Manual workflows	○	○	○	●	○

Any additional challenges?

Please complete challenges that are not mentioned above (optional).

Do you write code to automate the data analysis process?

- ● Yes
- ○ No

Do you program/set up a new/custom data processing workflows?

- [ ] Yes
- [x] No

How long does it take to set up such a process?

depending on the data and product scope, about 2-5 days

Can you optimise your data analysis operations?

On what kind of infrastructure(s) do you usually run the analysis:

- [ ] cluster
- [ ] high spec workstation
- [ ] HPC
- [x] personal laptop
- [x] server

INFORE solutions

Which INFORE data sources would be useful for you for the MSA Use Case and would be useful for you:

- [ ] Acoustic data
- [x] AIS data
- [x] Satellite imagery
- [ ] Thermal Camera data

Other data sources?

Which events would you like to extract from these data sources?

- [x] Normal vessel activities (fishing, transshipments, tugging, piloting, etc.)
- [x] Illegal vessel activities (smuggling, illegal fishing, entering protected/prohibited areas, etc.)
- [ ] Other

Rate your satisfaction on the variety of maritime complex events that INFORE is able to forecast, accuracy and interpretability of results:

	1: Not at all	2: Very little	3: Neutral	4: Pretty much	5: Very much
How much are you satisfied by the variety of complex events that can be forecasted?					X
How much would you trust the output of the INFORE platform with respect to accuracy?				X	

To what extent do you understand the results presented to you?				X	

Are there specific events that you would like to forecast in real-time, which we currently cannot forecast? If so, please explain.

If the answer is "No", you can leave this field blank.

Rate the following objectives of INFORE, based on how useful they are at YOUR data analysis.

	1: Not useful	2: Little Use	3: Average Use	4: Quite useful	5: Very useful
Ability to design data processing workflows with no code required				X	
Ability to change algorithm parameters graphically				X	
Ability to receive quick approximate answers instead of 100% accurate, but long running queries				X	
Ability to interactively explore the data in order to detect patterns/features of interest					X
Ability to accurately forecast events of interest					X
over different data processing platforms (HPC, Big Data Platforms, etc).				X	

What is the expected added value from INFORE for you and your corporation. Rate from 1 (lowest priority) to 5 (highest priority).

You can assign each number to multiple options.

	1	2	3	4	5
Performance				X	
Ability to handle multiple sources				X	
Timely forecast of events				X	
Interactive and efficient optimizable workflows will save time and improve				X	
Automation of processes will reduce human error				X	

Overall evaluation

How likely would your organisation be to use the INFORE platform operationally in the future?	★★★★☆

How useful is the combination of data sources used in INFORE?	★★★★☆

☑ I have read and understood the information sheet, or it has been read to me. I have been given the opportunity and enough time to ask questions about the study and my questions have been fully answered.I agree voluntarily to be a participant in this study and understand that I can decide to withdraw from the study at any time.I understand that taking part in the study may involve audio-recorded interviews and I am willing to devote enough time to respond to the questionnaire.I give permission for the data that I provide to be de-identified and deposited in a repository so it can be used for INFORE's purposes as outlined above.I understand that personal information collected about me, will not be shared and only de-identified or aggregative information will be used for INFORE purposes.I understand that de-identified or aggregative information I provide may be used for reports and research outputs, possibly made available to websites and social media.

Terms and privacy policy

Responses you give in the questionnaires and interviews may be recorded. Your recorded data will be de-identified; hence it will not be possible to identify your identity afterwards. Information will be processed during the phase of requirement analysis and aggregative results may be presented in project reports. It will not be possible to identify the individual source (that is you) of the information. The aggregative results of this investigation may be published in scientific journals or conferences and may be used in further studies. No personal data will be handed out to third parties.You can request your information be deleted at any time, without giving a reason. If you should decide to deny your consent, please contact the Project Coordinator, Prof. Antonios Deligiannakis (adeli[at]imin.athena-innovation.gr) and let him know of your intention of leaving the study.Your participation in this study is only possible if you freely and independently agree to authorize the INFORE consortium to use the data you provide. With your consent, the data will be stored for the purposes described above until the end of the project (31/12/2021), when all data will be permanently deleted .

☑ I accept the terms and privacy policy described above.

Contact

konstantina.bereta@marinetraffic.com

Existing MSA workflows

Please describe the different kinds of data sources that you use in your day-to-day tasks and the tools that you use to process them

Marine Traffic AIS or pre-processed data

How many tools do you typically use to integrate or handle the different sources of data mentioned above

Python, MS SQL

What are the events you are trying to identify?

- [ ] fishing
- [ ] piloting
- [ ] smuggling
- [ ] trafficking
- [x] transshipments
- [ ] tugging

Any additional events you would like to identify?

Delays on reported destination

What data processing challenges do you experience in your day-to-day tasks (e.g., fusion of heterogeneous sources, performance, analytics)? Rate them starting from 1 (lowest priority) to 5 (highest priority).

Please use each priority number only once

	1	2	3	4	5
Streaming nature of data	○	●	○	○	○
Too much data	●	○	○	○	○
Different data formats	○	○	●	○	○
Manual workflows	○	○	○	●	○

Any additional challenges?

Please complete challenges that are not mentioned above (optional).

Do you write code to automate the data analysis process?

- ● Yes
- ○ No

Do you program/set up a new/custom data processing workflows?

- [x] Yes
- [ ] No

How long does it take to set up such a process?

Depends on the case, usually 1 or 2 weeks

Can you optimise your data analysis operations?

Depends on the case

On what kind of infrastructure(s) do you usually run the analysis:

- [x] cluster
- [ ] high spec workstation
- [ ] HPC
- [x] personal laptop
- [x] server

INFORE solutions

Which INFORE data sources would be useful for you for the MSA Use Case and would be useful for you:

- [ ] Acoustic data
- [x] AIS data
- [x] Satellite imagery
- [ ] Thermal Camera data

Other data sources?

Which events would you like to extract from these data sources?

- [x] Normal vessel activities (fishing, transshipments, tugging, piloting, etc.)
- [ ] Illegal vessel activities (smuggling, illegal fishing, entering protected/prohibited areas, etc.)
- [ ] Other

Rate your satisfaction on the variety of maritime complex events that INFORE is able to forecast, accuracy and interpretability of results:

	1: Not at all	2: Very little	3: Neutral	4: Pretty much	5: Very much
How much are you satisfied by the variety of complex events that can be forecasted?					X
How much would you trust the output of the INFORE platform with respect to accuracy?					X

To what extent do you understand the results presented to you?	○	○	○	○	●

Are there specific events that you would like to forecast in real-time, which we currently cannot forecast? If so, please explain.

If the answer is "No", you can leave this field blank.

Rate the following objectives of INFORE, based on how useful they are at YOUR data analysis.

	1: Not useful	2: Little Use	3: Average Use	4: Quite useful	5: Very useful
Ability to design data processing workflows with no code required	○	○	○	○	●
Ability to change algorithm parameters graphically	○	○	○	●	○
Ability to receive quick approximate answers instead of 100% accurate, but long running queries	○	○	○	○	●
Ability to interactively explore the data in order to detect patterns/features of interest	○	○	○	○	●
Ability to accurately forecast events of interest	○	○	○	○	●
over different data processing platforms (HPC, Big Data Platforms, etc).	○	○	○	●	○

What is the expected added value from INFORE for you and your corporation. Rate from 1 (lowest priority) to 5 (highest priority).

You can assign each number to multiple options.

	1	2	3	4	5
Performance	○	○	○	●	○
Ability to handle multiple sources	○	○	○	○	●
Timely forecast of events	○	○	○	●	○
Interactive and efficient optimizable workflows will save time and improve	○	○	○	○	●
Automation of processes will reduce human error	○	○	○	○	●

Overall evaluation

How likely would your organisation be to use the INFORE platform operationally in the future?	★★★★☆

How useful is the combination of data sources used in INFORE?	★★★★★

☑ I have read and understood the information sheet, or it has been read to me. I have been given the opportunity and enough time to ask questions about the study and my questions have been fully answered.I agree voluntarily to be a participant in this study and understand that I can decide to withdraw from the study at any time.I understand that taking part in the study may involve audio-recorded interviews and I am willing to devote enough time to respond to the questionnaire.I give permission for the data that I provide to be de-identified and deposited in a repository so it can be used for INFORE's purposes as outlined above.I understand that personal information collected about me, will not be shared and only de-identified or aggregative information will be used for INFORE purposes.I understand that de-identified or aggregative information I provide may be used for reports and research outputs, possibly made available to websites and social media.

Terms and privacy policy

Responses you give in the questionnaires and interviews may be recorded. Your recorded data will be de-identified; hence it will not be possible to identify your identity afterwards. Information will be processed during the phase of requirement analysis and aggregative results may be presented in project reports. It will not be possible to identify the individual source (that is you) of the information. The aggregative results of this investigation may be published in scientific journals or conferences and may be used in further studies. No personal data will be handed out to third parties.You can request your information be deleted at any time, without giving a reason. If you should decide to deny your consent, please contact the Project Coordinator, Prof. Antonios Deligiannakis (adeli[at]imin.athena-innovation.gr) and let him know of your intention of leaving the study.Your participation in this study is only possible if you freely and independently agree to authorize the INFORE consortium to use the data you provide. With your consent, the data will be stored for the purposes described above until the end of the project (31/12/2021), when all data will be permanently deleted .

☑ I accept the terms and privacy policy described above.

Contact

konstantina.bereta@marinetraffic.com